EPA-600/4-75-016b
December 1975

Environmental Monitoring Series

TURBULENCE MODELING AND ITS APPLICATION TO ATMOSPHERIC DIFFUSION
Part II

Environmental Sciences Research Laboratory
Office of Research and Development
U.S. Environmental Protection Agency
Research Triangle Park, N.C. 27711

RESEARCH REPORTING SERIES

Research reports of the Office of Research and Development, U.S. Environmental Protection Agency, have been grouped into five series. These five broad categories were established to facilitate further development and application of environmental technology. Elimination of traditional grouping was consciously planned to foster technology transfer and a maximum interface in related fields. The five series are:

1. Environmental Health Effects Research
2. Environmental Protection Technology
3. Ecological Research
4. Environmental Monitoring
5. Socioeconomic Environmental Studies

This report has been assigned to the ENVIRONMENTAL MONITORING series. This series describes research conducted to develop new or improved methods and instrumentation for the identification and quantification of environmental pollutants at the lowest conceivably significant concentrations. It also includes studies to determine the ambient concentrations of pollutants in the environment and/or the variance of pollutants as a function of time or meteorological factors.

This document is available to the public through the National Technical Information Service, Springfield, Virginia 22161.

EPA-600/4-75-016b
December 1975

TURBULENCE MODELING AND ITS APPLICATION TO ATMOSPHERIC DIFFUSION
PART II: CRITICAL REVIEW OF THE USE OF INVARIANT MODELING

by

W. S. Lewellen and M. Teske
Aeronautical Research Associates of Princeton, Inc.
Princeton, New Jersey 08540

Contract No. 68-02-1310

Project Officer

Kenneth L. Calder
Meteorology and Assessment Division
Environmental Sciences Research Laboratory
Research Triangle Park, North Carolina 27711

U.S. ENVIRONMENTAL PROTECTION AGENCY
OFFICE OF RESEARCH AND DEVELOPMENT
ENVIRONMENTAL SCIENCES RESEARCH LABORATORY
RESEARCH TRIANGLE PARK, NORTH CAROLINA 27711

DISCLAIMER

This report has been reviewed by the Environmental Sciences Research Laboratory, U.S. Environmental Protection Agency, and approved for publication. Approval does not signify that the contents necessarily reflect the views and policies of the U.S. Environmental Protection Agency, nor does mention of trade names or commercial products constitute endorsement or recommendation for use.

TECHNICAL REPORT DATA
(Please read Instructions on the reverse before completing)

1. REPORT NO. EPA-600/4-75-016b	2.	3. RECIPIENT'S ACCESSION NO.
4. TITLE AND SUBTITLE TURBULENCE MODELING AND ITS APPLICATION TO ATMOSPHERIC DIFFUSION. PART II: CRITICAL REVIEW OF THE USE OF INVARIANT MODELING		5. REPORT DATE December 1975
		6. PERFORMING ORGANIZATION CODE
7. AUTHOR(S) W. S. Lewellen and M. Teske		8. PERFORMING ORGANIZATION REPORT NO. A.R.A.P. Report 254, Part II
9. PERFORMING ORGANIZATION NAME AND ADDRESS Aeronautical Research Associates of Princeton, Inc. 50 Washington Road Princeton, New Jersey 08540		10. PROGRAM ELEMENT NO. 1AA009
		11. CONTRACT/GRANT NO. EPA 68-02-1310
12. SPONSORING AGENCY NAME AND ADDRESS Environmental Sciences Research Laboratory Office of Research and Development U.S. Environmental Protection Agency Research Triangle Park, North Carolina 27711		13. TYPE OF REPORT AND PERIOD COVERED Interim
		14. SPONSORING AGENCY CODE EPA-ORD

15. SUPPLEMENTARY NOTES

Issued as Part II of 2 Parts

16. ABSTRACT

A method for the calculation of turbulent shear flows based on closure of the equations for second-order correlations of fluctuating quantities is reviewed. Various model possibilities for closure are described and detailed evaluation of coefficients for a simple model is outlined. Comparisons of model predictions and experimental data for a wide variety of laboratory and atmospheric flows are presented.

17. KEY WORDS AND DOCUMENT ANALYSIS

a. DESCRIPTORS	b. IDENTIFIERS/OPEN ENDED TERMS	c. COSATI Field/Group
* Turbulence * Turbulent flow * Atmospheric diffusion * Mathematical models		12A 20D 04A

18. DISTRIBUTION STATEMENT RELEASE TO PUBLIC	19. SECURITY CLASS *(This Report)* UNCLASSIFIED	21. NO. OF PAGES 55
	20. SECURITY CLASS *(This page)* UNCLASSIFIED	22. PRICE

EPA Form 2220-1 (9-73)

PREFACE

This critical review of our A.R.A.P. turbulence model was presented as a three-hour lecture in the one-week course, "Fundamentals and Applications of Turbulence," at the University of Tennessee Space Institute, Tullahoma, Tennessee, during the week of April 21-25, 1975. It includes a discussion of the development, validation tests, limitations, and some of the applications of the model. The work reviewed has been supported by a number of government agencies over the past four years. In addition to EPA support since 1971, the work has been partially supported by NASA, AFOSR, and the Navy in addition to internal corporate support. Detailed contractual acknowledgements are provided in the referenced reports.

TABLE OF CONTENTS

		Page
	Preface	ii
	Abstract	1
1.	Introduction	1
2.	Model Development	2
	1. Closure Requirements	2
	2. Dissipation Terms	4
	3. Pressure Correlations	5
	4. Third-Order Velocity Correlations	7
	5. Modeled Equations	8
	6. Scale Determination	9
3.	Evaluation of Model Coefficients	12
	1. Dissipation Coefficient (b)	12
	2. Diffusion Coefficient (v_c)	13
	3. Scale Determination	13
	4. Low Reynolds Number Dependence (a)	16
	5. Additional Coefficients Required to Compute Temperature Fluctuations (A, s, s_5)	16
4.	Model Verification	18
	1. Axisymmetric Free Jet	19
	2. Free Shear Layer	20
	3. Two-Dimensional Wake	21
	4. Axisymmetric Wake	21
	5. Flat Plate Boundary Layer	22
	6. Flow Over an Abrupt Change in Surface Roughness	27
	7. Temperature Fluctuations in the Plane Turbulent Wake	27
	8. Stability Influence in the Atmospheric Surface Layer	27
	9. Shear Layer Entrainment in a Stratified Fluid	31
	10. Free Convection	31
	11. Planetary Boundary Layer for Neutral Steady State	33
5.	Local Equilibrium Approximations	34
6.	Applications	37
	1. Diurnal Variations in the Planetary Boundary Layer	38
	2. Stratified Wake	39
	3. Pollutant Dispersal	41

7. Concluding Remarks 42
References 43

USE OF INVARIANT MODELING

W. S. Lewellen
Aeronautical Research Associates of Princeton, Inc.
Princeton, New Jersey

Abstract

A method for the calculation of turbulent shear flows based on closure of the equations for second-order correlations of fluctuating quantities is reviewed. Various model possibilities for closure are described and detailed evaluation of coefficients for a simple model is outlined. Comparisons of model predictions and experimental data for a wide variety of laboratory and atmospheric flows are presented.

1. Introduction

Previous lectures in this series have contained several different methods for calculating turbulent flow with varying degrees of complexity and probable computational success. Here I will describe the development and some applications of a method which has been pursued by Donaldson and his colleagues at A.R.A.P. for several years. The name of the model, an invariant model, can be interpreted in two ways. It refers to the constraints imposed on the choice of model terms required for closure. That is, any model term must exhibit the same tensor symmetry and dimensionality as the term it replaces. But the goal of the approach can also be described as an invariant model in the sense that our goal is a model which,although it is semi-empirical, has no varying constants which must be determined for each new flow.

This review has been partially funded with federal funds from the Environmental Protection Agency under Contract No. EPA 68-02-1310. The content of this paper does not necessarily reflect the views or policies of the U.S. Environmental Protection Agency.

Our starting point is the exact equation for the Reynolds stress. In choosing to attempt closure at the level of the equations for the second-order correlations, we are assuming that this will yield a more general model than first-order closure does. Certainly the second-order equations contain a great deal of physical information regarding the dynamics of the turbulent fluctuations. Providing this information is not lost by inappropriate modeling of the terms required for closure, this approach should be more general than first-order closure. In fact, it will be seen in a later section that a relatively rational, first-order closure model is obtained as a subset of our invariant model.

No attempt will be made to give a complete review of the literature surrounding turbulence transport modeling. Some surveys have been given by Bradshaw,[1] Mellor and Herring,[2] and Reynolds.[3] A convenient collection of some of the most important literature has been made by Harlow.[4] I will attempt to relate the model described here to those under development by other investigators. A limited number of comparisons between the numerical results of various models will be made.

In Section 2, the requirements for closure are outlined and some of the various model choices that have been made by various investigators are presented. Following a discussion of the alternatives, a relatively simple second-order closure model is chosen. The determination of the required empirical coefficients is described in Section 3. Detailed comparisons between the simple model's predictions and available data are made in Section 4 for a wide spectrum of flows. Although there are discrepancies in some of the variables for some of the flows, the overall verification is highly encouraging. In Section 5, the simplfications to the transport equations under local equilibrium conditions are explored. As already mentioned, this provides a bridge between first- and second-order closure. Section 6 contains some of the results of calculations for three applications of practical interest: a stratified wake, diurnal variations in the planetary boundary layer, and pollutant dispersal in the atmosphere.

2. Model Development

2.1 Closure Requirements

When the flow variables are decomposed into a mean and a fluctuating quantity, the mean flow equations may be written as

$$\frac{\partial U_i}{\partial t} + U_j \frac{\partial U_i}{\partial x_j} = - \frac{\partial \overline{u_i u_j}}{\partial x_j} + \frac{\partial}{\partial x_j} \nu \frac{\partial U_i}{\partial x_j} - \frac{1}{\rho} \frac{\partial P}{\partial x_i} + \frac{g_i(\Theta - \Theta_0)}{\Theta} - 2\varepsilon_{ijk}\Omega_j U_k \tag{2.1}$$

$$\frac{\partial U_i}{\partial x_i} = 0 \tag{2.2}$$

$$\frac{\partial \Theta}{\partial t} + U_j \frac{\partial \Theta}{\partial x_j} = - \frac{\partial \overline{u_i \theta}}{\partial x_i} + \frac{\partial}{\partial x_i}\left(k \frac{\partial \Theta}{\partial x_i} \right) \tag{2.3}$$

The flow has been assumed incompressible but with small variations in density due to changes in temperature. Following the Boussinesq approximation,[5] the only effect of the density variation is in the gravitational body force term in the momentum equation (2.1). The last term in (2.1) is that due to coriolis forces present in a coordinate system rotating with angular velocity Ω. It is included here in anticipation of atmospheric applications. Equation (2.3) is a diffusion equation for the temperature perturbation.

This system of equations is not complete due to the presence of the Reynolds stress terms. Exact equations for these correlations of the fluctuating variables may be derived as outlined in the introductory lectures or by Donaldson.[6]

$$\begin{aligned}\frac{\partial \overline{u_i u_j}}{\partial t} + U_k \frac{\partial \overline{u_i u_j}}{\partial x_k} = & - \overline{u_i u_k} \frac{\partial U_j}{\partial x_k} - \overline{u_j u_k} \frac{\partial U_i}{\partial x_k} + \frac{g_i \overline{u_j \theta}}{\Theta} + \frac{g_j \overline{u_i \theta}}{\Theta} \\ & - 2\varepsilon_{ik\ell}\Omega_k \overline{u_\ell u_j} - 2\varepsilon_{j\ell k}\Omega_\ell \overline{u_k u_i} - \frac{\partial}{\partial x_k}(\overline{u_k u_i u_j}) \\ & - \overline{\frac{u_i}{\rho} \frac{\partial p}{\partial x_j}} - \overline{\frac{u_j}{\rho} \frac{\partial p}{\partial x_i}} + \nu \frac{\partial^2 \overline{u_i u_j}}{\partial x_k^2} - 2\nu \overline{\frac{\partial u_i}{\partial x_k} \frac{\partial u_j}{\partial x_k}}\end{aligned} \tag{2.4}$$

$$\begin{aligned}\frac{\partial \overline{u_i \theta}}{\partial t} + U_j \frac{\partial \overline{u_i \theta}}{\partial x_j} = & - \overline{u_i u_j} \frac{\partial \Theta}{\partial x_j} - \overline{u_j \theta} \frac{\partial U_i}{\partial x_j} + \frac{g_i \overline{\theta^2}}{\Theta} - 2\varepsilon_{ijk}\Omega_j \overline{u_k \theta} \\ & - \frac{\partial \overline{u_i u_j \theta}}{\partial x_j} - \overline{\frac{\theta}{\rho} \frac{\partial p}{\partial x_i}} - \nu\theta \frac{\partial^2 \overline{u_i}}{\partial x_j^2} - k\overline{u_i \frac{\partial^2 \theta}{\partial x_j^2}}\end{aligned} \tag{2.5}$$

$$\frac{\partial \overline{\theta^2}}{\partial t} + U_j \frac{\partial \overline{\theta^2}}{\partial x_j} = - 2\overline{u_j\theta} \frac{\partial \Theta}{\partial x_j} - \frac{\partial}{\partial x_j} \overline{u_j\theta^2} + k \frac{\partial^2 \overline{\theta^2}}{\partial x_j^2} - 2k \overline{\frac{\partial \theta}{\partial x_j} \frac{\partial \theta}{\partial x_j}} \qquad (2.6)$$

This still does not permit the system to close. In fact, for each new equation added, several more unknown flow variables are added. Clearly, continuing the process by deriving exact expressions for these correlations will add further new correlations in ever-increasing numbers. This is the closure problem.

Closure of the system of equations at the level of (2.4) to (2.6) is called second-order closure. In (2.4) this requires neglecting or modeling in terms of the other variables three terms:

$$\frac{\partial}{\partial x_k} (\overline{u_k u_i u_j}) \ , \ \left(\overline{\frac{u_i}{\rho} \frac{\partial p}{\partial x_j} + \frac{u_j}{\rho} \frac{\partial p}{\partial x_i}} \right) \ , \quad 2\nu \overline{\frac{\partial u_i}{\partial x_k} \frac{\partial u_j}{\partial x_k}} \qquad (2.7)$$

Let us consider these three terms in some detail. The analogous terms in (2.5) and (2.6) can then be modeled in a similar manner.

2.2 Dissipation Terms

The last term in (2.7) measures the effect of viscous decay on the structure of the Reynolds stresses. Even in high Reynolds number flow, we expect viscous dissipation to be the major loss mechanism for turbulent kinetic energy. Due to the nonlinear terms in the Navier-Stokes equation, a reduction in viscosity is compensated by a reduction in scale of the smallest eddies in the flow. The turbulent dissipation process is often compared to that of a cascading waterfall with energy flowing from the mean flow to ever-decreasing scale eddies. The cascade continues until a scale sufficiently small to permit viscosity to dissipate the energy as heat is reached. When the dissipation eddies are much smaller than the eddies which receive their energy directly from the mean flow (i.e., when the Reynolds number is large), one may assume that they are statistically independent of the mean flow geometry. The scale of these isotropic dissipative eddies can then only depend on the dissipation rate ε and the viscosity ν. This Kolmogorov microscale[7] is

$$\eta = (\nu^3/\varepsilon)^{1/4} \qquad (2.8)$$

Just as the end of the cascade contains no information on the scale of the large eddies, the breakup rate of the large eddies should be independent of ν . Therefore, for high Reynolds number, it appears dimensionally correct to have

$$\varepsilon = \nu \overline{\frac{\partial u_i}{\partial x_k} \frac{\partial u_i}{\partial x_k}} \sim q^3/\Lambda \tag{2.9}$$

where q is the rms value of the total velocity fluctuation and Λ is a macroscale of the eddies. Since the viscous dissipation process is an isotropic process, most investigators model the dissipation terms as an isotropic term; i.e.,

$$\nu \overline{\frac{\partial u_i}{\partial x_k} \frac{\partial u_j}{\partial x_k}} = C_1 \delta_{ij} \frac{q^3}{\Lambda} \tag{2.10}$$

Some[8,9,10] have modeled it as an anisotropic term. A form which goes to (2.10) in the limit of $Re \to \infty$, but reflects the probability that at low Re dissipation will be anisotropic, is

$$\nu \overline{\frac{\partial u_i}{\partial x_k} \frac{\partial u_j}{\partial x_k}} = C_1 \delta_{ij} \frac{q^3}{\Lambda} + \frac{C_2}{\Lambda^2} \overline{u_i u_j} \tag{2.11}$$

The first term of the form adopted in (2.11) corresponds to taking the Taylor microscale λ proportional to $\Lambda/(a + bq\Lambda/\nu)^{1/2}$ where a and b are constants, as suggested by Rotta.[11]

Several investigators prefer to calculate ε from a dynamic equation obtained by modeling its governing equation. This will be discussed in Section 2.6 since, through (2.9), it is equivalent to an equation for Λ .

2.3 Pressure Correlations

The correlations involving pressure fluctuations are more difficult to model than the dissipation terms. These terms redistribute the turbulent energy produced by the leading term on the right-hand side of (2.4). This can perhaps be more readily seen by rewriting the pressure correlations as

$$\pi_{ij} = \overline{\frac{u_i}{\rho} \frac{\partial p}{\partial x_j}} + \overline{\frac{u_j}{\rho} \frac{\partial p}{\partial x_i}} = \overline{\frac{\partial u_i p}{\partial x_j}} + \overline{\frac{\partial u_j p}{\partial x_i}} - \overline{\frac{p}{\rho}\left(\frac{\partial u_i}{\partial x_j} + \frac{\partial u_j}{\partial x_i}\right)} \tag{2.12}$$

Since the flow is incompressible, there will be no contribution from the last term in (2.12) to the kinetic energy of the turbulence, $q^2/2 = \overline{u_i u_i}/2$. It contributes only to a

redistribution of energy between the Reynolds stresses. A volume integral of the first two terms on the right-hand side of (2.12) over any finite region of turbulence bounded by laminar flow will yield zero. Thus these two terms must only contribute to a spatial redistribution, i.e., are diffusion terms.

All investigators appear to follow Rotta[11] in modeling at least one contribution of the pressure correlation as a return-to-isotropy term proportional to the extent to which the flow is anisotropic; i.e.,

$$\pi_{ij} = \frac{C_3 q}{\Lambda}\left(\overline{u_i u_j} - \delta_{ij}\frac{q^2}{3}\right) \tag{2.13}$$

The term in parentheses, the departure from isotropy, provides the right tensor symmetry and q/Λ provides the correct dimensionality. Donaldson[6,8] adds to this a spatial diffusion term with proper symmetry and dimensionality to represent the first two terms on the right-hand side of (2.12):

$$\pi_{ij} = \frac{C_3 q}{\Lambda}\left(\overline{u_i u_j} - \delta_{ij}\frac{q^2}{3}\right) + C_4\left[\frac{\partial q\Lambda}{\partial x_i}\frac{\partial \overline{u_k u_j}}{\partial x_k} + \frac{\partial q\Lambda}{\partial x_j}\frac{\partial \overline{u_k u_j}}{\partial x_k}\right] \tag{2.14}$$

It is possible to show that the pressure correlation should probably depend on the mean flow strain. By taking the divergence of the fluctuating Navier-Stokes equations, a Poisson equation for p may be obtained:

$$\frac{1}{\rho}\nabla^2 p = -2\frac{\partial U_i}{\partial x_j}\frac{\partial u_j}{\partial x_i} - \frac{\partial^2}{\partial x_i \partial x_j}\left(u_i u_j - \overline{u_i u_j}\right) + \frac{g_i}{\Theta}\frac{\partial \theta}{\partial x_i} - 2\varepsilon_{ijk}\Omega_j\frac{\partial u_k}{\partial x_i} \tag{2.15}$$

Equation (2.15) can be formally integrated to obtain p which may then be differentiated and correlated with u_i to form π_{ij}. The integral cannot be solved so the procedure can only be used to suggest the form of the modeled term. The simplest addition to (2.14) to incorporate an influence of mean strain is a term of the form

$$C_5 q^2\left(\frac{\partial U_i}{\partial x_j} + \frac{\partial U_j}{\partial x_i}\right) \tag{2.16}$$

In fact, a numerical value for C_5 (= 0.2) has been obtained by Rotta[12] and by Crow[13] for the limiting case of isotropic turbulence in a weak, homogeneous mean strain. However, such a large value appears to make the term too overpowering for any practical calculations. A term such as (2.16) has been

included by several modelers[14, 15, 16] with C_5 empirically determined.

A form for the mean strain term with a good deal of appeal is that suggested by Launder[17]

$$C_5 \left(P_{ij} - \delta_{ij} \frac{P_{ii}}{3} \right) \tag{2.17}$$

where P_{ij} represents the production terms for the Reynolds stress in (2.4). A similar term is included in the more involved model of Naot et al.[18] Adding (2.17) to (2.14) would be equivalent to assuming that the pressure correlations not only drive the turbulence towards isotropy with a term linearly proportional to the departure from isotropy, but also redistribute the production terms with a term linearly proportional to the anisotropy of the production terms.

Neither (2.16) nor (2.17) is sufficient to account for the observation that the mean strain effect is often not symmetric between u_2 and u_3 when the flow is one-dimensional in the x_1 direction. More complicated model variations for the pressure correlation terms may be found in the work of Lumley and Khajeh-Nouri,[19] Hanjalic and Launder,[20] Wolfshtein, et al,[10] Zeman and Tennekes,[21] and Varma.[22]

2.4 Third-Order Velocity Correlations

This term represents a process by which the Reynolds stress is transferred from one part of the flow to another without any net production or loss. Again this can be demonstrated, as it was for the pressure diffusion term of (2.12), by integration over a finite volume. When the volume is bounded by either laminar or by homogeneous isotropic flow, the integral will vanish. The most popular modeling of this transport term is as gradient diffusion, although Bradshaw[1] has suggested that it could well be algebraic.

A number of different gradient diffusion forms have been used as a model for this term. Donaldson[8] proposed a form which satisfies the tensor symmetry of $\overline{u_k u_i u_j}$ with a scalar diffusion coefficient

$$D_{ij} = \frac{\partial}{\partial x_k} \left(\overline{u_k u_i u_j} \right) = C_5 \frac{\partial q\Lambda}{\partial x_k} \left(\frac{\partial \overline{u_i u_j}}{\partial x_k} + \frac{\partial \overline{u_k u_i}}{\partial x_j} + \frac{\partial \overline{u_k u_j}}{\partial x_i} \right) \tag{2.18}$$

Hanjalic and Launder[20] used a form with tensorial diffusivity

$$D_{ij} = C_5 \frac{\partial}{\partial x_k} \frac{\Lambda}{q} \left(\overline{u_k u_\ell} \frac{\partial \overline{u_i u_j}}{\partial x_\ell} + \overline{u_i u_\ell} \frac{\partial \overline{u_j u_k}}{\partial x_\ell} + \overline{u_j u_\ell} \frac{\partial \overline{u_i u_k}}{\partial x_\ell} \right) \tag{2.19}$$

They obtained this form by a "firm pruning" of the exact

equation for $\overline{u_k u_i u_j}$. The simplest possible form is given by

$$D_{ij} = C_5 \frac{\partial q\Lambda}{\partial x_k} \frac{\partial \overline{u_i u_j}}{\partial x_k} \tag{2.20}$$

Although this form satisfies the tensor symmetry of D_{ij}, it does not satisfy the symmetry of $\overline{u_k u_i u_j}$ itself.

Wolfshtein et al.[10] and Lumley and Khajeh-Nouri[19] propose forms that have considerably more terms and involve a number of coefficients. These currently appear to have too many coefficients for manageable computations.

2.5 Modeled Equations

Our philosophy here is to first attempt calculations with the simplest possible second-order closure models. We choose to use (2.11) for the dissipation term, (2.13) for the pressure velocity interaction, and the pressure contribution to diffusion incorporated with the velocity diffusion for one diffusion term like (2.20).

$$\nu \overline{\frac{\partial u_i}{\partial x_k} \frac{\partial u_j}{\partial x_k}} = \frac{b\delta_{ij} q^3}{3\Lambda} + \frac{a\nu \overline{u_i u_j}}{\Lambda^2} \tag{2.21}$$

$$\overline{\frac{p}{\rho}\left(\frac{\partial u_i}{\partial x_j} + \frac{\partial u_j}{\partial x_i}\right)} = -\frac{q}{\Lambda}\left(\overline{u_i u_j} - \delta_{ij}\frac{q^2}{3}\right) \tag{2.22}$$

$$\frac{\partial}{\partial x_k}\left(\overline{u_k u_i u_j}\right) + \frac{\partial \overline{u_i p}}{\partial x_j} + \frac{\partial \overline{u_j p}}{\partial x_i} = \nu_c \frac{\partial q\Lambda}{\partial x_k} \frac{\partial \overline{u_i u_j}}{\partial x_k} \tag{2.23}$$

In this restatement of the modeled terms, C_3 has been set equal to 1 by using (2.13) to define the macroscale Λ. The other coefficients have been assigned the symbols used in the most recent A.R.A.P. publications.

Equations (2.21) - (2.23) provide the minimum requirements of any second-order closure. The combination of terms in (2.21) and (2.22) provides a destruction term for each of the Reynolds stress components which allows an equilibrium value to be reached in a time long compared with Λ/q. The term in (2.23) prevents any excessively sharp gradients in Reynolds stresses from occurring.

When similar terms are used in the heat flux and temperature variance equations, (2.5) and (2.6), the modeled set of second-order correlation equations may be written as

$$\frac{\partial \overline{u_i u_j}}{\partial t} + U_k \frac{\partial \overline{u_i u_j}}{\partial x_k} = - \overline{u_i u_k} \frac{\partial U_j}{\partial x_k} - \overline{u_j u_k} \frac{\partial U_i}{\partial x_k} + \frac{g_i \overline{u_j \theta}}{\Theta} + \frac{g_j \overline{u_i \theta}}{\Theta}$$

$$- 2\varepsilon_{ik\ell}\Omega_k \overline{u_\ell u_j} - 2\varepsilon_{j\ell k}\Omega_\ell \overline{u_k u_i} + v_c \frac{\partial q\Lambda}{\partial x_k} \frac{\partial \overline{u_i u_j}}{\partial x_k}$$

$$- \frac{q}{\Lambda}\left(\overline{u_i u_j} - \delta_{ij} \frac{q^2}{3}\right) + \nu \frac{\partial^2 \overline{u_i u_j}}{\partial x_k^2}$$

$$- \delta_{ij} \frac{2bq^3}{3\Lambda} - \frac{2a\nu \overline{u_i u_j}}{\Lambda^2} \tag{2.24}$$

$$\frac{\partial \overline{u_i \theta}}{\partial t} + U_j \frac{\partial \overline{u_i \theta}}{\partial x_j} = - \overline{u_i u_j} \frac{\partial \Theta}{\partial x_j} - \overline{u_j \theta} \frac{\partial U_i}{\partial x_j} + \frac{g_i \overline{\theta^2}}{\Theta} - 2\varepsilon_{ijk}\Omega_j \overline{u_k \theta}$$

$$+ v_c \frac{\partial q\Lambda}{\partial x_j} \frac{\partial \overline{u_i \theta}}{\partial x_j} - \frac{Aq}{\Lambda} \overline{u_i \theta} + k \frac{\partial^2 \overline{u_i \theta}}{\partial x_j^2} + \frac{ak\overline{u_i \theta}}{\Lambda^2} \tag{2.25}$$

$$\frac{\partial \overline{\theta^2}}{\partial t} + U_j \frac{\partial \overline{\theta^2}}{\partial x_j} = - 2\overline{u_j \theta} \frac{\partial \Theta}{\partial x_j} + v_c \frac{\partial q\Lambda}{\partial x_j} \frac{\partial \overline{\theta^2}}{\partial x_j} + k \frac{\partial^2 \overline{\theta^2}}{\partial x_j^2} - \frac{2bsq\overline{\theta^2}}{\Lambda} \tag{2.26}$$

This is the set we choose to make calculations with here. Rather than use models with a large number of coefficients that are finely adjusted to fit a few particular flows, we choose to work with a relatively minimum number. Only as experience proves that more terms are required will other terms and coefficients be added. Two additional coefficients were included in (2.25) and (2.26), A and s. Both of these were first set equal to one,[6] but as will be seen in the next section, it was later found desirable to add flexibility.

2.6 Scale Determination

To complete closure, it is necessary to provide some means for determining the turbulent scale Λ involved in the modeled terms. This is approached in different ways by various investigators. It may be specified empirically based on the gross features of the particular flow geometry. Or it may be predicted from a semi-empirically modeled, dynamic differential equation. Each of these approaches has some advantages and disadvantages.

The macroscale Λ is defined by (2.21)-(2.23). It is expected to be related to the integral scale discussed in earlier lectures but, due to our choice of normalization, not equal to it. It is also related to the mixing length discussed in Deissler's lecture. As such, there is empirical information which can be used in our determination of this model parameter. It appears fairly clear that the scale cannot exceed some fraction of the total spread of the region of turbulence and that, in some neighborhood of the wall, it should be proportional to the distance from the wall. These two simple ideas, together with empirical information used to determine the two implied constants of proportionality, are sufficient to permit the system to close with relatively good numerical results for many problems.[6,23,24] Others[25,26] have specified a completely empirically determined distribution of Λ across the region of interest in the same manner as is done for first-order mixing length approaches.

In an attempt to remove some of the arbitrariness of the specification of Λ for different flows, a number of investigators have resorted to a modeled dynamic equation for Λ or its equivalent. The starting points for such attempts have varied widely. A two-point-velocity-correlation equation forms the basis for the work of Rotta,[12] Naot et al.[18] Donaldson,[6] and Rodi.[15] By forming an equation for the two-point velocity correlation $\overline{u_i(x)u_i(x+r)}$ and integrating to form an integral scale, it appears appropriate to take

$$q^2\Lambda = c\iiint_V \overline{u_i(x)u_i(x+r)}\,\frac{dv}{r^2} \tag{2.27}$$

For a flow without body forces, this leads to, following Wolfshtein,[10]

$$\begin{aligned}\frac{D(q^2\Lambda)}{Dt} = \iiint_V \Bigg\{ & [U_k(x) - U_k(x+r)]\,\frac{\partial\overline{u_i(x)u_i(x+r)}}{\partial r_k} \\ & - \overline{u_i(x)u_k(x+r)}\,\frac{\partial U_i(x+r)}{\partial x_k} + \overline{u_k(x)u_i(x+r)}\,\frac{\partial U_i(x)}{\partial x_k} \\ & - \frac{1}{c}\frac{\partial}{\partial x_k}\,\overline{u_k(x)u_i(x)u_i(x+r)} \\ & - \frac{1}{c}\frac{\partial}{\partial r_k}\,[\overline{u_i(x)u_k(x+r)u_i(x+r)} - \overline{u_i(x)u_k(x)u_i(x+r)}] +\end{aligned}$$

$$- \frac{1}{c\rho} \frac{\partial p(x) u_i(x+r)}{\partial x_i} - \frac{1}{c\rho} \frac{\partial}{\partial r_i} [\overline{u_i(x) p(x+r)} - \overline{p(x) u_i(x+r)}]$$

$$- \nu \frac{\partial^2}{\partial x_k^2} \overline{u_i(x) u_i(x+r)} - 2\nu \frac{\partial^2 \overline{u_i(x) u_i(x+r)}}{\partial x_k \partial r_k}$$

$$\left. + 2\nu \frac{\partial^2 \overline{u_i(x) u_i(x+r)}}{\partial r_k^2} \right\} \frac{dv}{r^2} \tag{2.28}$$

The difficulty with this approach is readily apparent. None of the terms on the right-hand side of (2.28) can be integrated exactly. All of the terms must be modeled. This is also true if one starts with the equation for the dissipation ε as is favored by many (e.g., Lumley and Khajeh-Nouri,[19] Harlow and Nakayama,[27] and Hanjalic and Launder [20]) or with the equation for the vorticity fluctuations as suggested by Daly and Harlow[9] or Wilcox and Alber.[28] With the model chosen in Section 2.5, $\varepsilon = bq^3/\Lambda$. Also the vorticity fluctuation can be taken as proportional to q/Λ . Thus with the aid of the energy equation, any of these approaches may be reduced to an equation for Λ . As Bradshaw[1] and Mellor and Herring[2] have pointed out, all of the resulting Λ equations have the same form

$$\frac{D\Lambda}{Dt} = - s_1 \frac{\Lambda}{q^2} \overline{u_i u_j} \frac{\partial U_i}{\partial x_j} - s_2 bq + \text{diffusion terms} \tag{2.29}$$

The difference in the various expressions lies in the construction of the turbulent diffusion terms. Unfortunately, these turn out to be more important in the scale equation than in the Reynolds stress equation. The scale equation we have experimented with at A.R.A.P.[29,30] starts with a rather general diffusion term of the form

$$\text{diffusion terms} = s_0 \frac{\partial}{\partial x_i} \left(v_c q\Lambda \frac{\partial \Lambda}{\partial x_i} \right) + s_3 \frac{\Lambda}{q^2} \frac{\partial}{\partial x_i} \left(q\Lambda \frac{\partial q^2}{\partial x_i} \right)$$

$$+ s_4 q \left(\frac{\partial \Lambda}{\partial x_i} \right)^2 + s_6 \frac{\Lambda}{q^2} \left(\frac{\partial q}{\partial x_i} \right)^2 + s_7 \frac{\partial q}{\partial x_i} \frac{\partial \Lambda}{\partial x_i} \tag{2.30}$$

As pointed out by Mellor and Herring[2] this covers the possibility of starting with equations for the quantity $q^m \Lambda^n$ and in combination with the energy equation reducing it to (2.29). As in the formulations of Refs. 6 and 9, we will add a term

proportional to $(\Lambda/q^2)g_i\overline{u_i\theta}/\Theta$ to permit the direct effect of stratification.

It is immediately obvious that the scale equation contains much more arbitrariness than the Reynolds stress equations where many of the terms were determined precisely without recourse to modeling or coefficients. With such a large number of coefficients in the scale equation, a correspondingly large number of different experiments must be matched concurrently if the resulting coefficients are to have any invariant validity.

There is also the question as to what extent it is really appropriate to have the integral quantity Λ determined by point values of the other variables. It seems that spatial boundary conditions may be expected to play a much more important role in the determination of Λ than they do for the Reynolds stress.

3. Evaluation of Model Coefficients

With the exception of the model scale variable Λ, the simple model chosen in Section 2.5 contains five coefficients: a, b, v_c, A, and s. Ideally these coefficients should be constants, but conceptually the approach is still valid if they turn out to be unique functions of the dimensionless parameters. For the flow specified in (2.1)-(2.3), there are three such dimensionless parameters: a Reynolds number, a Richardson number, and a Rossby number. The coefficients might also be a function of some dimensionless number characterizing the state of the turbulence, such as that proposed by Lumley and Khajeh-Nouri[19]

$$(\overline{u_iu_j} - \delta_{ij}q^2/3)(\overline{u_ju_i} - \delta_{ji}q^2/3)/q^4$$

We will initially, optimistically, assume that the coefficients are constant. If the coefficients have to be functions of the dimensionless variables, then the second-order approach will lose some of its advantage over first-order closure. Insofar as is possible, each coefficient should be determined from a critical flow experiment that involves only that coefficient.

3.1 Dissipation Coefficient (b)

For high Reynolds number turbulence, the most sensitive model coefficient in (2.24) is the coefficient b. The value of this coefficient can be isolated by considering steady, homogeneous turbulence with no body forces. When a one-dimensional mean flow in the x_1 direction is considered with a gradient in only one direction, x_3, (2.24) reduces to

$$0 = -\overline{u_i u_3}\frac{\partial U_1}{\partial x_3}\delta_{1j} - \overline{u_j u_3}\frac{\partial U_1}{\partial x_3}\delta_{1i} - \frac{q}{\Lambda}\left(\overline{u_i u_j} - \delta_{ij}\frac{q^2}{3}\right) - \delta_{ij}\frac{2bq^3}{3\Lambda} \tag{3.1}$$

From these separate component equations, one can obtain several different expressions for b independent of Λ.

$$b = \frac{\overline{u_1 u_3}^2}{\overline{u_3 u_3}\, q^2} = \frac{3}{2}\left(\frac{1}{3} - \frac{\overline{u_3 u_3}}{q^2}\right) = \frac{3}{2}\left(\frac{1}{3} - \frac{\overline{u_2 u_2}}{q^2}\right) \tag{3.2}$$

The data of Champagne et al.[31] for such a homogeneous shear flow in a wind tunnel yield values of 0.12, 0.14, and 0.08, respectively, for the three expressions in (3.2). With the exception of the last value, these are all close to the value of 1/8 chosen by Donaldson[8] by comparison with other data. A closer fit to all the data will require additional model terms as discussed in Section 2.3.

The computational results to be described here have all been made with $b = 0.125$.

3.2 Diffusion Coefficient (v_c)

The diffusion coefficient v_c is difficult to decouple from the determination of the scale Λ. We have chosen a value of 0.3 based on computer studies of jets and wakes.[23] However, due to the relative insensitivity of our results to this coefficient, it is considered known only to $\pm.05$. This is the basic reason we have chosen to use the simplest form of diffusion, as given in (2.23). Critical measurements may show one of the more complicated forms to be preferable. The difficulty of measuring the pressure correlation contribution to diffusion makes the diffusion terms particularly difficult to isolate empirically. The best chance for finer detailed modeling of those terms probably lies in the possibility of detailed comparisons with ensemble averages from the type of simulated turbulence calculation described in Orzsag's lecture.

3.3 Scale Determination

Section 2.6 discussed two approaches to the determination of Λ. Let us first determine the two constants needed to fix the bounds on Λ. Close to a wall, we will assume $\Lambda = \alpha z$ with z the distance normal to the wall. The coefficient α is related directly to von Kármán's constant κ. In the "constant flux," surface layer region of a flat plate boundary layer, (3.1) holds with the subscript 1 denoting the direction

of the free stream flow and $x_3 = z$. When the definition of κ

$$\kappa = \left[\frac{z}{u^*}\frac{\partial U}{\partial z}\right]^{-1} \tag{3.3}$$

is used to eliminate the mean flow gradient, (3.1) can be arranged to yield

$$\alpha = \kappa b \left[\frac{b(1 - 2b)}{3}\right]^{-3/4} \tag{3.4}$$

With our previously assigned value of $b = 0.125$, (3.4) yields

$$\alpha = 1.68\kappa \tag{3.5}$$

The generally accepted value of κ from laboratory flows is 0.40, but rather extensive measurements in the atmospheric surface layer at much higher Reynolds numbers[32] give $\kappa = 0.36$. The corresponding values of α are 0.67 and 0.60. We have used 0.65 in most of the calculations to follow, although some have been performed with $\alpha = 0.60$.

The other bound of Λ is that tied to the spread of the region. This we have picked by computer optimization. For an axisymmetric wake or jet, it is 0.20 times the radius at which the turbulent energy falls to one-fourth its maximum value. For a two-dimensional boundary layer or wake, it is 0.3 times the similar measure of the turbulent spread. For a two-dimensional shear layer, it might be expected to be 0.6. It is clear that the more complicated the flow geometry is, the more difficult it becomes to specify Λ .

The second approach is an attempt to circumvent this difficulty by using a dynamic Λ equation with coefficients that are independent of flow geometry. Let us attempt to determine the coefficients in (2.29) and (2.30).

The coefficient s_2 can be estimated from the decay of homogeneous grid turbulence. If homogeneous turbulence is assumed to decay as

$$q^2 \sim x^{-n} \tag{3.6}$$

then from the contraction of (3.1)

$$\Lambda = bq^3 \Big/ \left(-\frac{1}{2} U \frac{\partial q^2}{\partial x}\right) \tag{3.7}$$

Equation (2.29) then leads to

$$s_2 = -\frac{U}{bq}\frac{\partial \Lambda}{\partial x} = -\frac{(2-n)}{n} \tag{3.8}$$

A recent review of grid turbulence experiments by Gad-el-Hak &

Corrsin[33] shows values of n predominantly between 1 and 1.3 with more of the values lying near 1.25. This value of n gives a value of $s_2 = -0.6$.

To reduce the number of diffusion coefficients, it is desirable to keep the coefficient of the direct diffusion term s_0 the same as in the Reynolds stress equation. This calls for $s_0 = 1$. It is compatible with this assumption to take $s_3 = 0$, since with $s_0 = 1$ any combination of m and n for an expression of the form

$$\frac{Dq^m\Lambda^n}{Dt} - v_c \frac{\partial}{\partial x_i}\left(q\Lambda \frac{\partial q^m\Lambda^n}{\partial x_i}\right) \tag{3.9}$$

would lead to an equation for $D\Lambda/Dt$ with $s_3 = 0$.

A simple relationship between s_0, s_1, s_2, and s_4 may be obtained from the reduced form of the scale equation in the steady, neutral, constant shear stress layer near a solid boundary where $\Lambda = \alpha z$. In this region, the scale equation reduces to

$$0 = s_1 \frac{\alpha z u^{*2}}{q^2} \frac{\partial U}{\partial z} - s_2 bq + v_c q\alpha^2 + s_4 q\alpha^2 \tag{3.10}$$

which, with the aid of the energy equation, may be reduced to

$$- s_4 = v_c + (b/\alpha^2)(s_1 - s_2) \tag{3.11}$$

This leaves s_1, s_6, and s_7 to be determined by computer optimization. Prior to doing this, we must determine boundary conditions for the scale.

The boundary conditions on the scale equation are not as straightforward as those on the Reynolds stress equations, since the scale need not go to zero at the free boundary of a region of turbulence. In fact, the eddies extending the farthest are expected to be the largest eddies present in the region. At a free boundary, we therefore set Λ equal to twice the bound established by the previous approach to Λ.

The edge boundary condition appears simpler if one chooses to use the dissipation equation, since $\varepsilon = bq^3/\Lambda$ clearly approaches zero. However, this leaves Λ free to approach any value from zero to infinity as $q \to 0$, and no independent information is gained.

Since the production term is small for a momentumless wake,[22] this provides a flow for estimating s_6 and s_7 to lie between 0.3 and 1. To reduce the uncertainty in these coefficients, we have rather arbitrarily set $s_4 = s_6 = s_7/2$.

The last coefficient, s_1, may now be determined by computer fit with the free jet result to be $\approx -.35$. This is in the middle of the range of values used by Rodi[15] who found it necessary to vary his analogous coefficient from 1.2 to 2 (corresponding to varying s_1 in our case from -1 to 0.6).

With these choices for the coefficients, our proposed scale equation for no body forces becomes

$$\frac{D\Lambda}{Dt} = 0.35 \frac{\Lambda}{q^2} \overline{u_i u_j} \frac{\partial U_i}{\partial x_j} + 0.6 \frac{\nu}{\lambda^2} \Lambda + 0.3 \frac{\partial}{\partial x_i} q\Lambda \frac{\partial \Lambda}{\partial x_i} - \frac{0.375}{q} \left(\frac{\partial q\Lambda}{\partial x_i} \right)^2 \tag{3.12}$$

As noted earlier, we cannot assign as high a confidence level to this equation as to our modeled Reynolds stress equations. In fact, it appears that unless the turbulence is far out of equilibrium, the approach of simply limiting the Λ to be equal to the lower of the two bounds previously described is adequate for a simple model.

3.4 Low Reynolds Number Dependence (a)

The coefficient a in (2.24) is only important at low Reynolds numbers, i.e., when $bq\Lambda/a\nu \leq O(1)$. The best measured low Reynolds turbulent flow is the transition region in a boundary layer just outside the so-called laminar sublayer. In this region, (2.1) reduces to

$$-\overline{u_1 u_3} + \nu \frac{\partial U_1}{\partial x_3} = \text{constant} = u_*^2 \tag{3.13}$$

Equation (3.13) and the four nonzero Reynolds stress component equations from (2.24) may be solved in this region and compared to Cole's empirical law of the wall.[34] This is done in Figure 3.1 for three values of a for the previously chosen values of α, b, and v_c. The best choice appears to be $a = 3$.

3.5 Additional Coefficients Required to Compute Temperature Fluctuations (A, s, s_5)

The coefficient A in (2.25) can be determined by again considering the constant flux region of a high Reynolds number boundary layer with no body forces, i.e., the limit of small temperature fluctuations. The normal component of (2.25) then reduces to

$$-\overline{u_3 u_3} \frac{\partial \Theta}{\partial x_3} - \frac{Aq}{\Lambda} \overline{u_3 \theta} = 0 \tag{3.14}$$

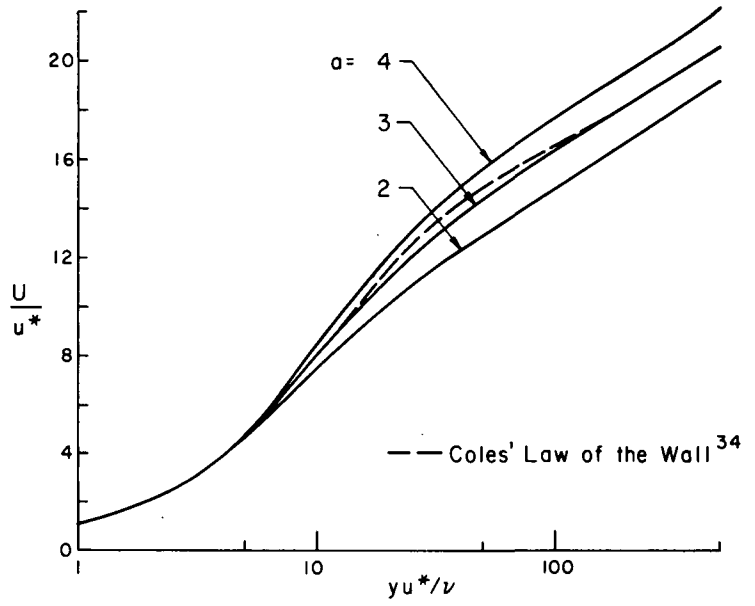

Fig. 3.1 Influence of a on model predictions of law of the wall

while the shear stress equation from (3.1) for the same conditions reduces to

$$-\overline{u_3u_3}\,\frac{\partial U_1}{\partial x_3} - \frac{q}{\Lambda}\,\overline{u_1u_3} = 0 \tag{3.15}$$

Equations (3.14) and (3.15) may be used to form the ratio of eddy diffusivity for momentum to that for heat. This is sometimes called the turbulent Prandtl number

$$Pr_t = \frac{\overline{u_1u_3}\,\dfrac{\partial\Theta}{\partial x_3}}{\overline{u_3\theta}\,\dfrac{\partial U_1}{\partial x_3}} = A \tag{3.16}$$

Based on the measurements of Businger et al.[32] in the neutral atmospheric surface layer, we chose a value of 0.75 for this coefficient.

The coefficient of the temperature dissipation term s can be evaluated by comparing the frequency spectrum of the temperature fluctuations with the spectrum of the turbulent kinetic energy. In the inertial subrange, it is experimentally observed that the three-dimensional energy spectrum in scalar wave-number space is given by[7]

$$E(k) = \alpha\varepsilon^{2/3}k^{-5/3} \tag{3.17}$$

with α a constant.

The temperature variance spectrum is similarly given by

$$E_\theta(k) = \beta N\varepsilon^{-1/3}k^{-5/3} \tag{3.18}$$

with β a constant and N the dissipation of temperature variance. By integrating (3.17) to form $q^2/2$ and (3.18) to form $\overline{\theta^2}/2$, it is possible to show that the coefficient s in (2.26) should be equated to α/β. With the values of $\alpha = 1.5$ and $\beta = 0.5$ given by Tennekes and Lumley[7] this would yield $s = 3.0$. But some values of the ratio are quoted as low as 0.6.[35] We have chosen a value of 1.8.[36] Mellor[16] chooses a value of 15/8 while Wyngaard et al.[37,38] chose a value of 2.8.

An estimate for the coefficient of the stratification term in the scale equation can be obtained from the stable, constant flux layer, for Richardson number equal to its critical value ≈ 0.21.[32] Assuming Λ and q constant, and picking the value of Λ that leads to $Ri_c = 0.21$,[36] we find a coefficient of 0.8 on the buoyancy term. Thus the form of the scale equation used here is

$$\frac{D\Lambda}{Dt} = 0.35\,\frac{\Lambda}{q^2}\,\overline{u_i u_j}\,\frac{\partial U_i}{\partial x_j} + 0.6\,\frac{\nu\Lambda}{\lambda^2} + 0.3\,\frac{\partial q\Lambda}{\partial x_i}\,\frac{\partial\Lambda}{\partial x_i} - \frac{0.375}{q}\left(\frac{\partial q\Lambda}{\partial x_i}\right)^2 + \frac{0.8\Lambda}{q^2}\,\frac{g_i\overline{u_i\theta}}{\Theta} \tag{3.19}$$

4. Model Verification

In viewing the comparisons between model predictions and experiments in this section, the reader should remember our goal of making reasonable predictions for a wide class of flows rather than very accurately predicting any one flow. Flows for which significant discrepancies occur between model predictions and observations for some of the variables will be noted. If one is interested in a relatively narrow class of flows, these discrepancies could be reduced by changes in the model coefficients. A better general model would require more sophisticated modeling of the individual terms, as discussed in Section 2.

4.1 Axisymmetric Free Jet

Comparisons between model predictions and the experimental data of Wygnanski and Fiedler[39] for the self-similar region of an axisymmetric free jet are given in Figure 4.1. The computations have been made[23,30] by starting with some arbitrary velocity and turbulence distributions and letting the jet develop until self-similar distributions are obtained. The model predictions have been made using both of the approaches to the scale determination discussed in Sections 2.6 and 3.3. The scale variations for the two approaches are compared with the measured longitudinal integral scale in Figure 4.1(c). The variation predicted by (3.12) is closer to the observations as expected, but the improvement, if any, in the predicted flow variables is not significant. The fact that the predicted energy is low while the predicted shear stress is high is the

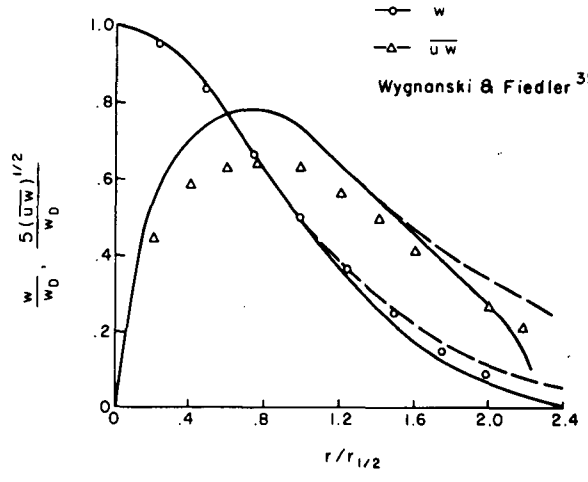

Fig. 4.1 Similarity profiles for axisymmetric free jet with constant Λ (—) and dynamic Λ (---);
(a) mean velocity and shear stress

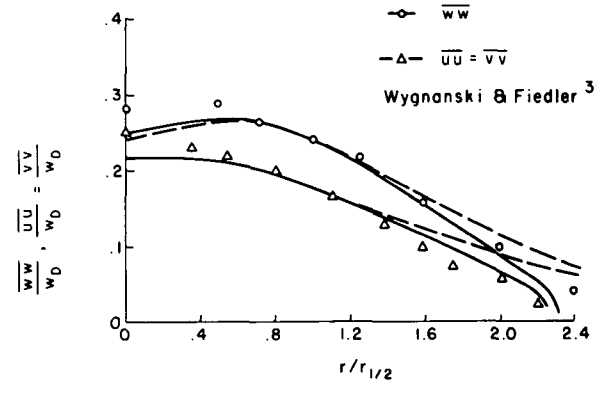

(b) normal Reynolds stress components

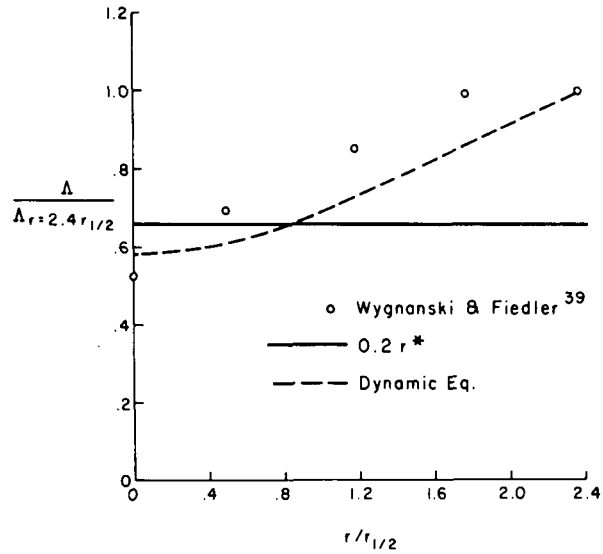

Fig. 4.1(c) scale variation

type of discrepancy one might expect to overcome by incorporating additional terms to the model of pressure correlations discussed in Section 2.3.

4.2 Free Shear Layer

Results for a two-dimensional, self-similar shear layer are compared with observations[40,41] in Figure 4.2. The agreement with the mean flow profile is good, but there exists

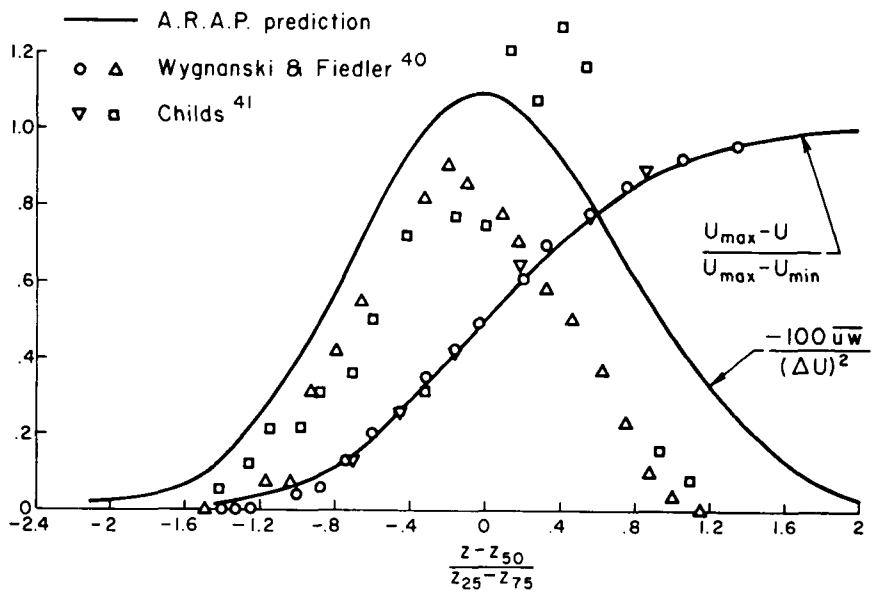

Fig. 4.2 Similarity profiles for free shear layer

considerable scatter in the data for the shear stress distribution. The components of the normal stress predicted by the model were compared with Wygnanski and Fiedler's data by Donaldson.[6] Because of some uncertainty surrounding the data,[41] these comparisons are not shown here.

4.3 Two-Dimensional Wake

Predictions are compared with Townsend's[42] self-similar wake measurements in Figure 4.3. Lumley and Khajeh-Nouri's[19] model predictions are also included for comparison. Their

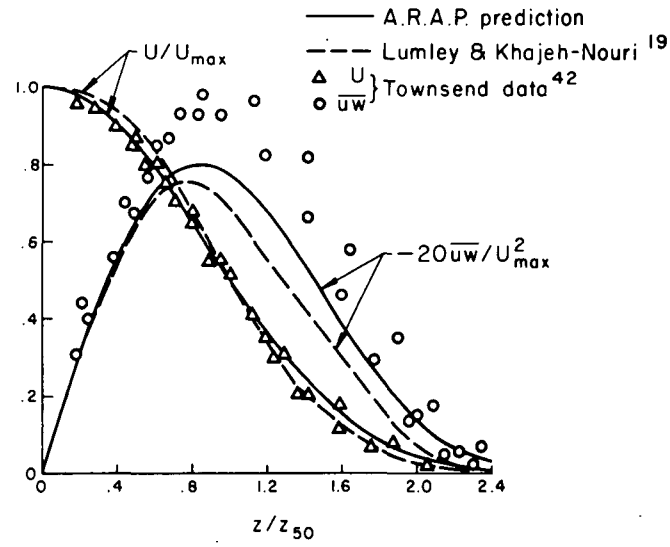

Fig. 4.3 Similarity profiles for two-dimensional wake; (a) mean velocity and shear stress

model, which contains many more terms and coefficients, makes a marginally better prediction for the normal components of the Reynolds stress for this flow. The lateral and transverse velocity fluctuations are equal in the present model predictions while the observations are significantly different.[43] Again, there is some uncertainty in the data since Thomas reports measurements of the longitudinal rms turbulence intensity which are about 33% higher than Townsend's reported values.

4.4 Axisymmetric Wake

The capability of the model to predict the development of a wake was tested by matching the velocity and Reynolds stress distributions as observed by Chevray[44] at one axial station and then comparing the predicted and observed development.[23] The decay of the maximum velocity defect w_D , the maximum shear stress uw_{max} , and the maximum axial velocity fluctuation

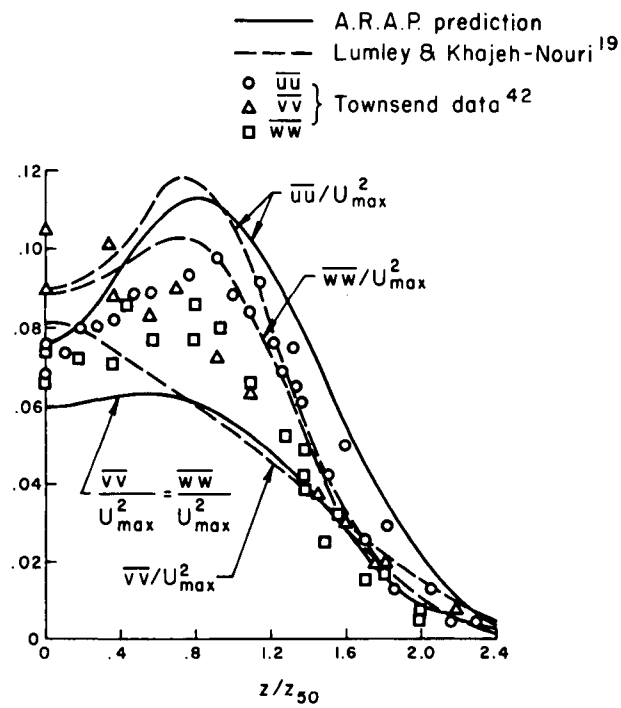

Fig. 4.3(b) normal Reynolds stress components

$\overline{ww}_{max}$ are given in Figure 4.4. The largest discrepancy is in the decay of the axial velocity fluctuations. The model predicts an increase of 35% over the initial value at $z/D = 3$ which the observations do not show.

The wake spread as measured by the radius for which the defect in the mean velocity is equal to half of its maximum value is given in Figure 4.5. The agreement is good. Although Chevray fits a 1/3-power law growth rate to his data eighteen diameters behind the body, the model indicates that ≈ 100 diameters is required for the wake to reach self similarity. The self-similar profiles obtained by the model are compared in Figures 4.6(a) and (b).

Comparisons between predictions and the momentumless wake measurements of Naudascher[45] have also been made[23] with results similar to the comparisons shown here with Chevray's measurements. In this case, no true self similarity exists.

4.5 Flat Plate Boundary Layer

Predicted velocity distributions in the neighborhood of the wall were compared with Coles' law of the wall[34] in Figure 3.1 in order to choose (a). Comparison with Klebanoff's[46] velocity and Reynolds stress measurements are given in Figure 4.7 for a Reynolds number of 5×10^6. The agreement with U

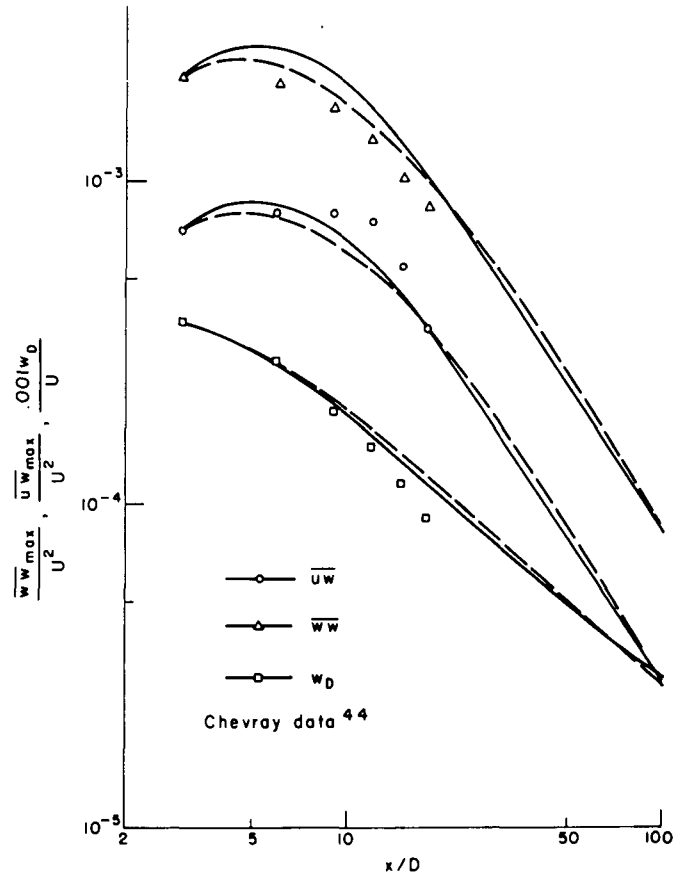

Fig. 4.4 Downstream decay of axisymmetric wake with constant Λ (—) and dynamic Λ (--)

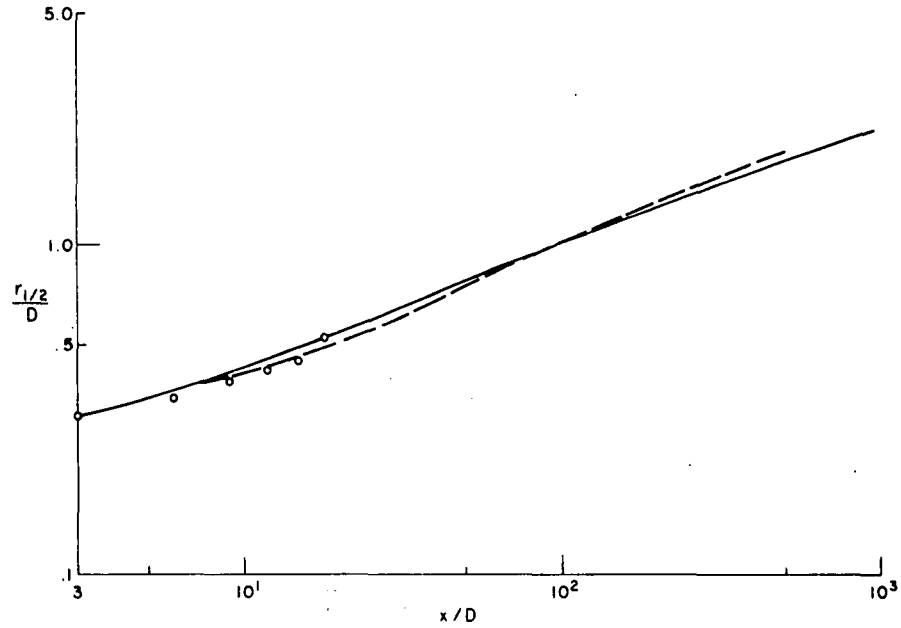

Fig. 4.5 Wake radius growth for conditions of Figure 4.4

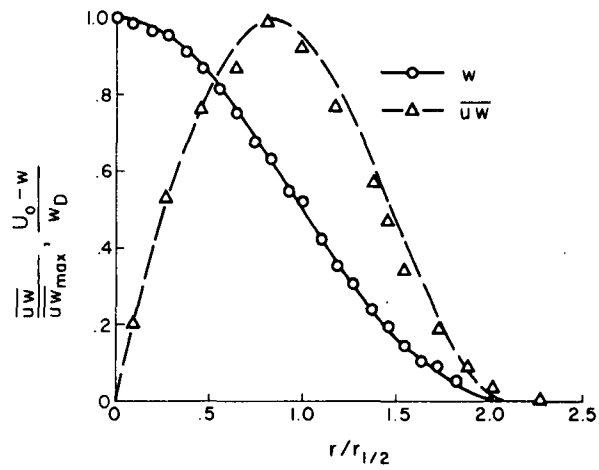

Fig. 4.6 Similarity profiles for conditions of Figure 4.4; (a) velocity defect and shear stress

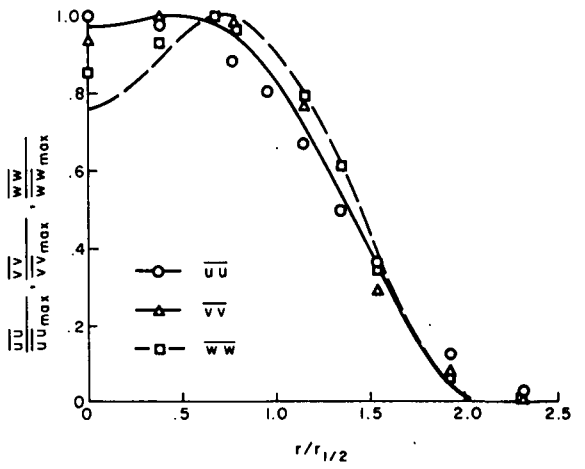

Fig. 4.6(b) normal Reynolds stress components

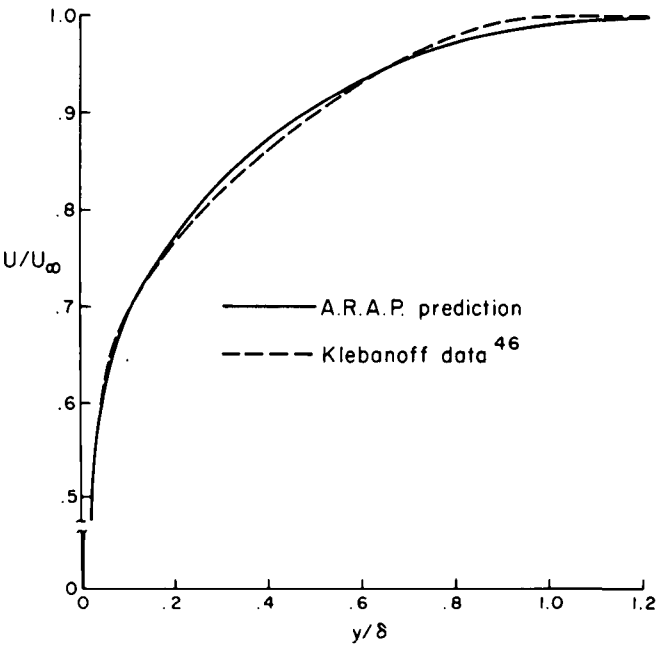

Fig. 4.7 Similarity profiles for flat plate boundary layer
(a) mean velocity

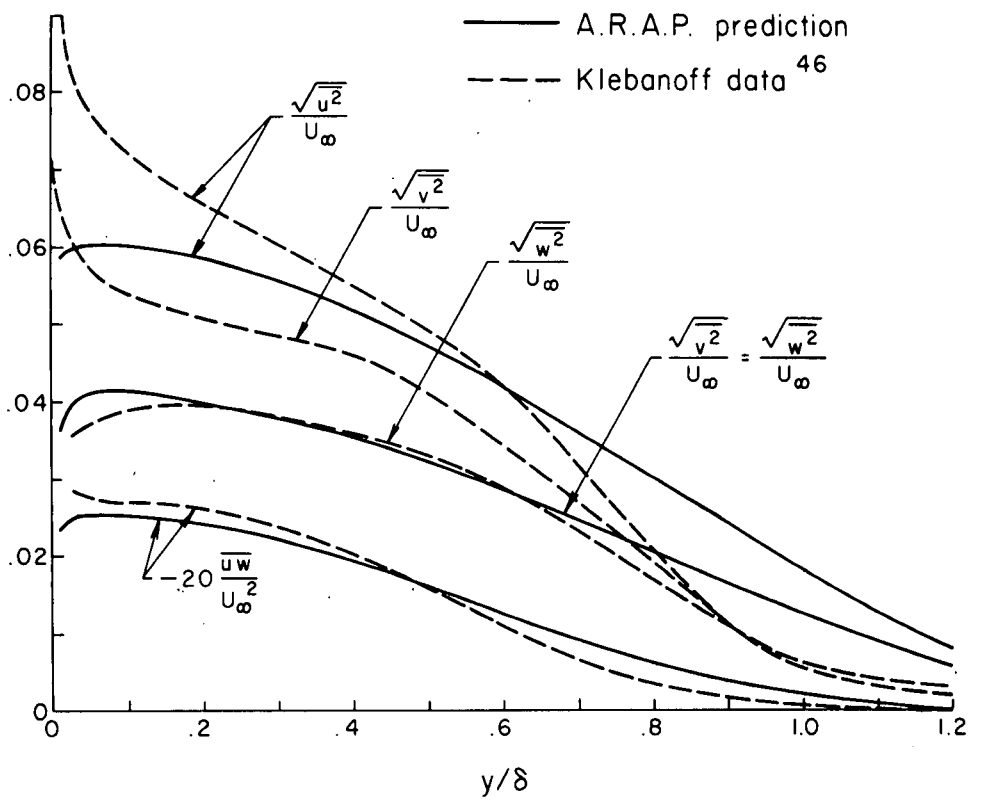

Fig. 4.7(b) Reynolds stress components

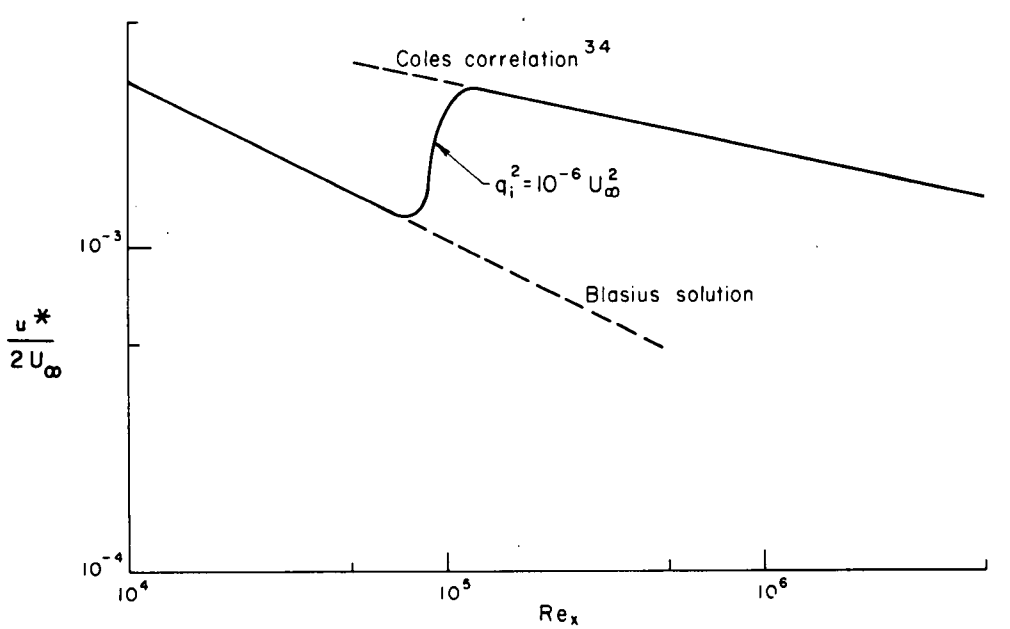

Fig. 4.8 Surface shear stress on a flat plate

and $\overline{uw}$ is good but the sharp peaks observed in $\overline{uu}$ and $\overline{vv}$ very near the wall are not predicted. There also appears to be a little too much diffusion in the outer region.

A plot of surface shear stress versus Reynolds number ($Re_x = Ux/\nu$) is given in Figure 4.8 along with the laminar, Blasius value, and Coles[34] compilation for fully turbulent flow. For this comparison, the calculation is started with the laminar velocity profile at a relatively small value of Re_x. All turbulent correlations are initially zero except for a small spot of turbulent energy. The model does a creditable job at predicting transition.

4.6 Flow Over an Abrupt Change in Surface Roughness

A calculation was made in simulation of the atmospheric surface data of Bradley[47] who recorded velocities and surface shear stress at a little-used airfield in Australia. Transitions are shown in Figure 4.9 for rough-to-smooth and smooth-to-rough, with the roughness measured in terms of the aerodynamic roughness z_0. The calculations[29] begin with the velocity and turbulence components in equilibrium for one value of z_0. The surface boundary condition is changed to that appropriate for the other value of z_0 at $x = 0$. When both runs are allowed to continue far downstream, the turbulence comes into equilibrium with the new z_0 value. Figure 4.9 also includes the predictions of Rao et al.[48] who used the second-order closure model developed in Reference 38.

4.7 Temperature Fluctuations in the Plane Turbulent Wake

Measurements behind a slightly heated cylinder have been made by Freymuth and Uberoi[49] and LaRue and Libby.[50] Figure 4.10 shows a comparison between the measured distributions far downstream of the cylinder and the self-similar profiles predicted by the model. The normalizing length z_{50} is fixed for the mean velocity profile given in Figure 4.3. The agreement is quite good, particularly in the concurrence of the amplitude and position of the maximum temperature fluctuation.

4.8 Stability Influence in the Atmospheric Surface Layer

The atmospheric surface layer extending a few tens of meters above the earth's surface is the most extensively studied example of a turbulent shear layer incorporating the influence of stratification on the dynamics of turbulence. Following Monin and Obukhov,[51] considerable success has been achieved in experimentally determining similarity functions which describe the dependence of the mean turbulence characteristics on height, shear stress, and heat flux. In this layer, the shear stress and heat flux may be considered constant.

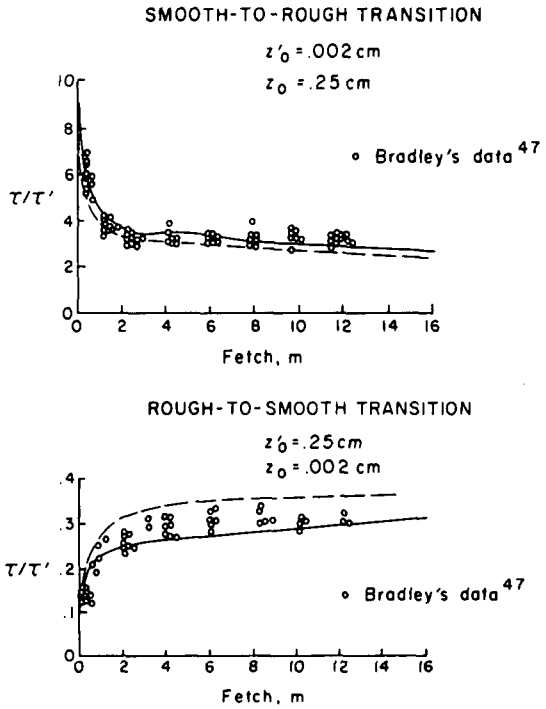

Fig. 4.9 Step change in surface roughness. A.R.A.P. prediction (—); prediction by Rao et al.[48] (---)

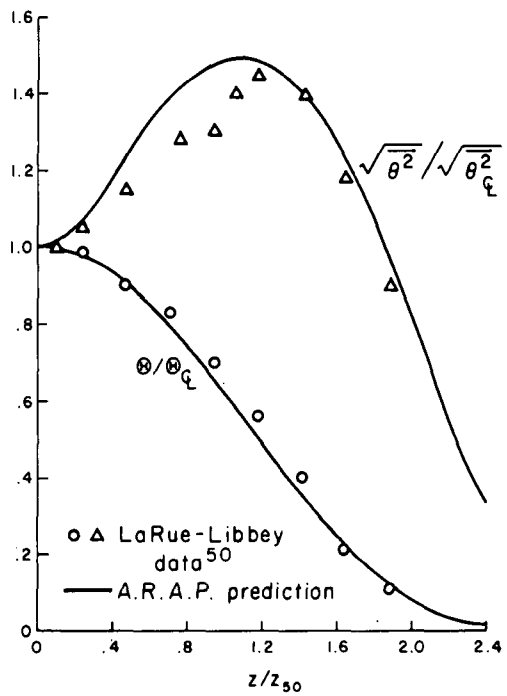

Fig. 4.10 Temperature similarity profiles in a two-dimensional wake

From these turbulent transport constants, a characteristic length may be found

$$L = -\frac{\Theta u_*^3}{kg\overline{w\theta}}$$

This is the Monin-Obukhov length. At altitudes below which any crossflows appear due to the coriolis force caused by the earth's rotation and above which the direct viscous contributions to momentum transport are important, z/L is the only variable determining the normalized turbulence quantities for a steady homogeneous layer. Equations (2.24)-(2.26) have been integrated for this case by Lewellen and Teske.[36] Results for the normalized wind and temperature gradients are compared with atmospheric data in Figure 4.11.

In these computations, the scale was set equal to $0.6z$ with an upper bound of $0.20L$ in stable flow. This was chosen to yield the observed critical Richardson number of 0.21. That is, no matter how stable the flow becomes in terms of large z/L, Ri never exceeds 0.21. This bound was also used in determining the coefficient of the buoyant term in the scale equation in Section 3.3.

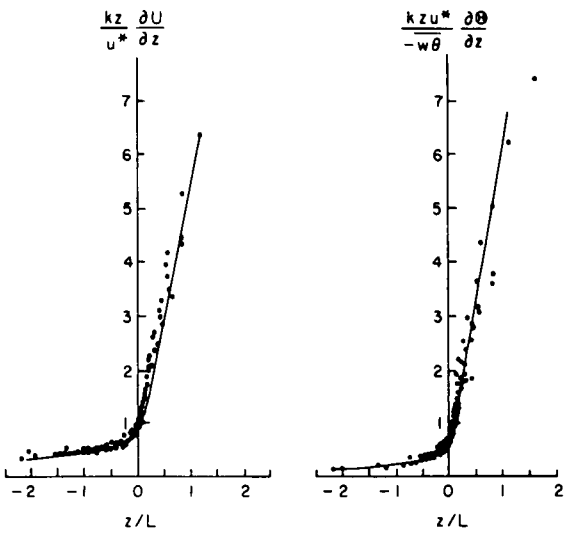

Fig. 4.11 Normalized atmospheric surface layer gradients as a function of stability. Data from Businger et al.[32]

The vertical velocity and temperature fluctuations are compared with the data of Wyngaard et al.[52] in Figures 4.12 and 4.13. The agreement for the vertical velocity is very good but that for the temperature fluctuations leaves a bit to be desired. As pointed out by Wyngaard et al.[52] there is

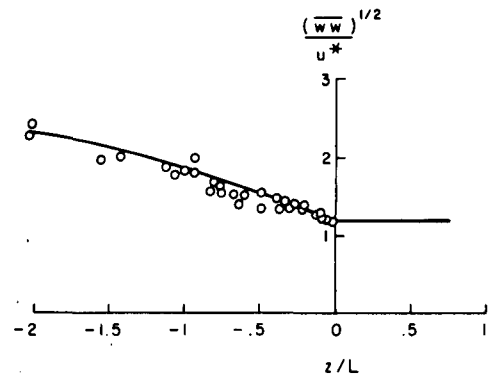

Fig. 4.12 Vertical velocity fluctuation in the atmospheric surface layer. Data from Wyngaard et al.[52]

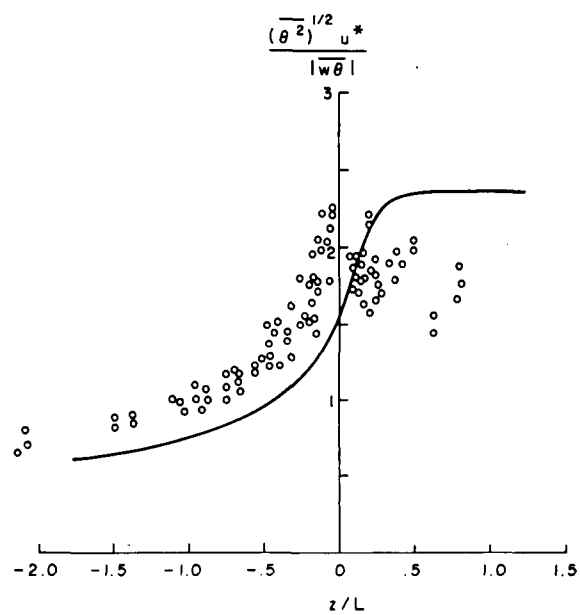

Fig. 4.13 Temperature fluctuation in the atmospheric surface layer. Data from Wyngaard et al.[52]

considerable uncertainty in $(\overline{\theta^2})^{1/2}/\overline{w\theta}$ at $z/L = 0$ because both variables go to zero.

Mellor[16] made a somewhat similar calculation of these surface layer similarity functions. The major difference is that Mellor eliminated the diffusion terms so that the differential equations reduce to an algebraic set. In this case the length scale may be normalized out of the problem, eliminating any need for, or any possibility of, incorporating an influence of stratification on the scale. His model coefficients

must then be chosen so that they will match the critical Richardson number.

4.9 Shear Layer Entrainment in a Stratified Fluid

Kato and Phillips[53] measured turbulent entrainment in an annular tank of density-stratified water with a shear stress applied at the surface by a rectangular mesh screen. The rate of spreading of the turbulent fluid into the linear density field was measured visually by injected dye. Their experimental results of entrainment rate versus flow Richardson number are given in Figure 4.14. The two model prediction curves[30] in the figure represent calculations using the two different approaches to the scale discussed in Section 2.6. The dynamic scale rounds the apparently straight-line prediction of the gross scale model. Neither model predicts quite as steep a decrease of entrainment with Richardson number as the data indicate.

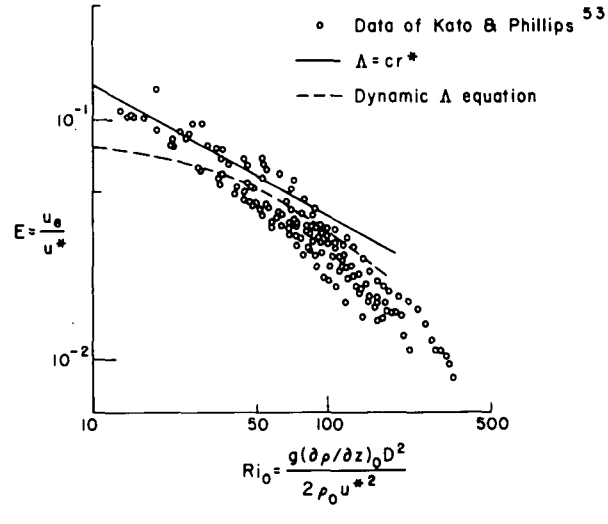

Fig. 4.14 Shear layer entrainment into a stratified fluid

4.10 Free Convection

Willis and Deardorff[54] have measured the velocity and temperature fluctuations in an unstable layer bounded above by a stable density gradient and below by a surface with a positive heat flux. Their experiment called for establishing an initial stable temperature gradient between two surfaces and then applying a heat flux to the region through the lower surface. With mean velocities restricted to a minimum, free convection occurs in a mixed layer above the lower surface. The thickness of this mixed layer increases with time, but the

fluctuating velocity distributions exhibit self-similarity when normalized by the characteristic velocity

$$w^* = \left(\frac{g\overline{w\theta}_0 z_i}{\Theta} \right)^{1/3}$$

where $\overline{w\theta}_0$ is the surface heat flux and z_i is the depth of the mixed layer.

Figure 4.15 shows our model predictions for the normalized vertical velocity fluctuations and the experimental observations. For the model predictions, we assumed no mean velocity to simulate the laboratory experiment and a constant surface heat flux. The agreement between predictions and observations is heartening, particularly since no model constant adjustments were involved.

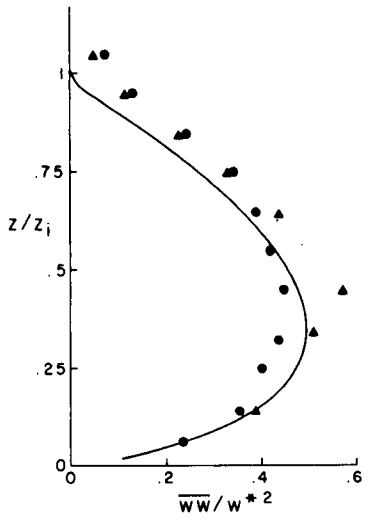

Fig. 4.15 Similarity profile of vertical velocity fluctuation in an unstable mixed layer. Data from Willis and Deardorff[54]

The horizontal velocity fluctuations are given in Figure 4.16. Here the comparison with experiment is not as close since the observations show a peak near the lower surface that is not evidenced in the model results. The distributions of temperature fluctuations are shown in Figure 4.17. The agreement between model and experiment is very good except at the top of the mixed layer where the observations show a much stronger local maximum than is predicted. This may be due to the fact that inertial oscillations exist in this region. Overall, the comparison between model predictions and experimental observations is quite favorable.

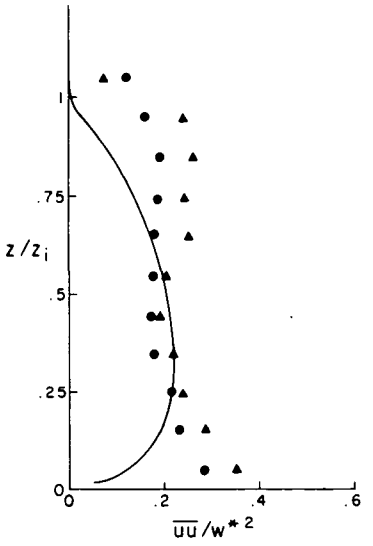

Fig. 4.16 Horizontal velocity fluctuations for the conditions of Figure 4.15

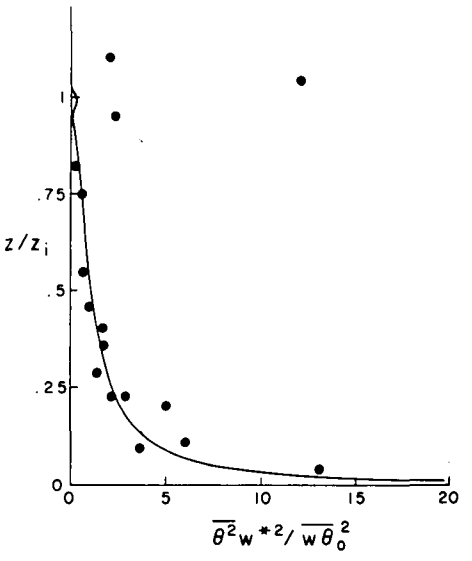

Fig. 4.17 Temperature fluctuations for the conditions of Figure 4.15

4.11 Planetary Boundary Layer for Neutral Steady State

Height variation of the mean velocities and Reynolds stress components is given in Figure 4.18 as predicted by our model for the atmospheric Ekman layer. The distributions are compared with Deardorff's[55] results of ensemble averages of integrations of the unsteady equations of motion for all the turbulent fluctuations above a prescribed grid size. The mean

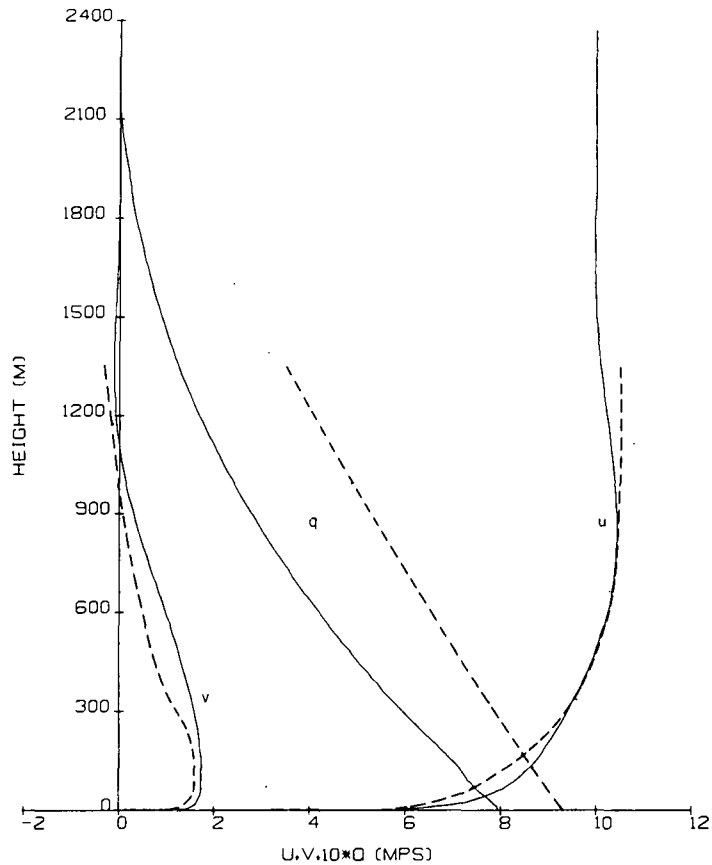

Fig. 4.18 Steady neutral atmospheric boundary layer profiles. A.R.A.P. prediction (—); prediction from Deardorff[55] (--)

velocity distributions are in good agreement. The value of the surface shear stress (u_*/U_g = .036) is within the scatter of field data for the same value of Rossby number. At the surface q is 14% lower than Deardorff's result for the same value of u*. A large part of this discrepancy occurs in the lateral velocity fluctuations. This tends to reinforce the need for some refinement of our pressure correlation modeling, as previously discussed. Near the top of the boundary layer, it appears that the accuracy of Deardorff's results is affected by his choice of a low value for his fixed boundary layer height.

5. Local Equilibrium Approximations

If the second-order correlations are assumed to be in local equilibrium so that there is no time evolution or spatial diffusion of the correlations, (2.24)-(2.26) may be reduced to

$$0 = -\overline{u_i u_k}\frac{\partial U_j}{\partial x_k} - \overline{u_j u_k}\frac{\partial U_i}{\partial x_k} + \frac{g_i\overline{u_j\theta}}{\Theta} + \frac{g_i\overline{u_i\theta}}{\Theta}$$

$$- 2\varepsilon_{ik\ell}\Omega_k\overline{u_\ell u_j} - 2\varepsilon_{j\ell k}\Omega_\ell\overline{u_k u_i} - \frac{q}{\Lambda}\left(\overline{u_i u_j} - \delta_{ij}\frac{q^2}{3}\right)$$

$$- \delta_{ij}\frac{2bq^3}{3\Lambda} \tag{5.1}$$

$$0 = -\overline{u_i u_j}\frac{\partial\Theta}{\partial x_j} - \overline{u_j\theta}\frac{\partial U_i}{\partial x_j} + \frac{g_i\overline{\theta^2}}{\Theta} - 2\varepsilon_{ijk}\Omega_j\overline{u_k\theta} - \frac{Aq\overline{u_i\theta}}{\Lambda} \tag{5.2}$$

$$0 = -2\overline{u_j\theta}\frac{\partial\Theta}{\partial x_j} - \frac{2bsq\overline{\theta^2}}{\Lambda} \tag{5.3}$$

The laminar terms have also been neglected since low Reynolds number is incompatible with equilibrium turbulence. Equations (5.1)-(5.3) form a closed set of algebraic relationships between the second-order correlations and the gradients of the mean velocity and temperature. This is what Donaldson[6] calls the superequilibrium approximation.

The relationships between the second-order correlations and the mean flow gradients determined by (5.1)-(5.3) form a first-order closure or K theory for turbulence. This will be a valid approximation, provided 1) any changes in the mean flow are very slow compared with the characteristic time of the turbulence Λ/q and 2) spatial variations in the turbulence are small over the scale length Λ. Note that only rarely are both conditions satisfied because Λ is usually related to spatial variations in the flow. One particular region where both conditions are satisfied is in the constant flux region of the boundary layer when Λ/q is approaching zero.

The functional dependence of the correlations on the mean flow gradients obtained from (5.1)-(5.3) for the case where $U_i = (U(z),0,0)$; $g_i = (0,0,-g)$; and $\Theta = \Theta(z)$ is shown in Figure 5.1. The only independent variable is the Richardson number of the mean flow

$$Ri = \frac{g}{\Theta}\frac{\partial\Theta}{\partial z}\Big/\left(\frac{\partial U}{\partial z}\right)^2$$

A critical Ri is reached, above which no turbulence can exist. This critical value of 0.56 given in Figure 5.1 is higher than the value 0.21 observed in the atmospheric surface layer by Businger et al.[32] as reported in Section 4. However,

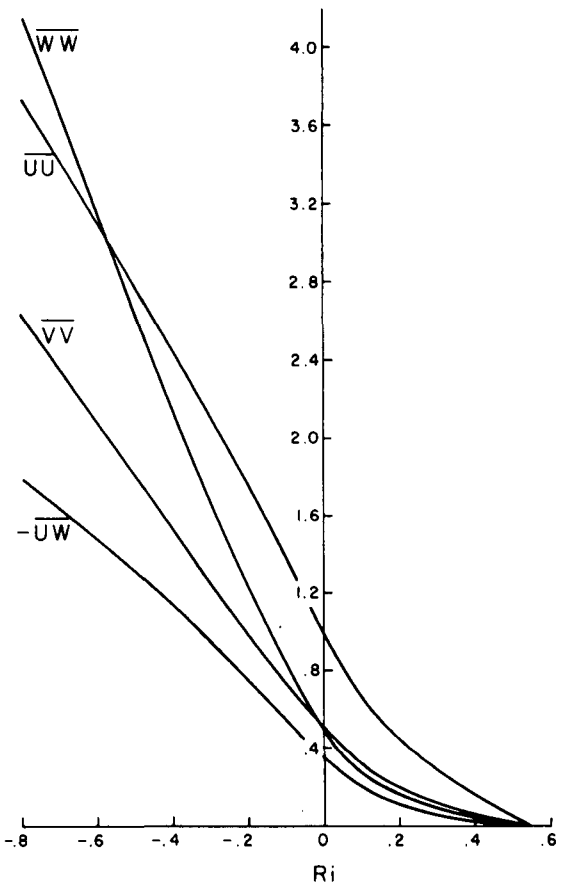

Fig.5.1(a) Superequilibrium Reynolds stress profiles normalized by $\Lambda^2(\partial U/\partial z)^2$

in this surface layer, the turbulent correlations vary with height as stability varies with height, so one should expect the diffusion terms to have some influence.

Superequilibrium relationships have also been computed for constant density swirling flows.[56,57,58] In this case, there is both a lower bound and an upper bound on the range of values the swirl parameter may have for turbulence to exist.

Other approximations to (2.24)-(2.26) may be tried short of reducing them to (5.1)-(5.3). Mellor and Yamada[26] have experimented with four levels of approximation. We have had some success with a type of energy equation approach we call quasi-equilibrium.[24,30] This consists of carrying the energy equation formed by the contraction of (2.24) in full but using (5.1)-(5.3) to relate the individual turbulent correlations to q^2 . This should be considerably more accurate than super-

equilibrium because overall levels of time evolution and spatial diffusion are included through the turbulent energy equation. It cannot accurately predict flows when the transport of a quantity is counter to its gradient.

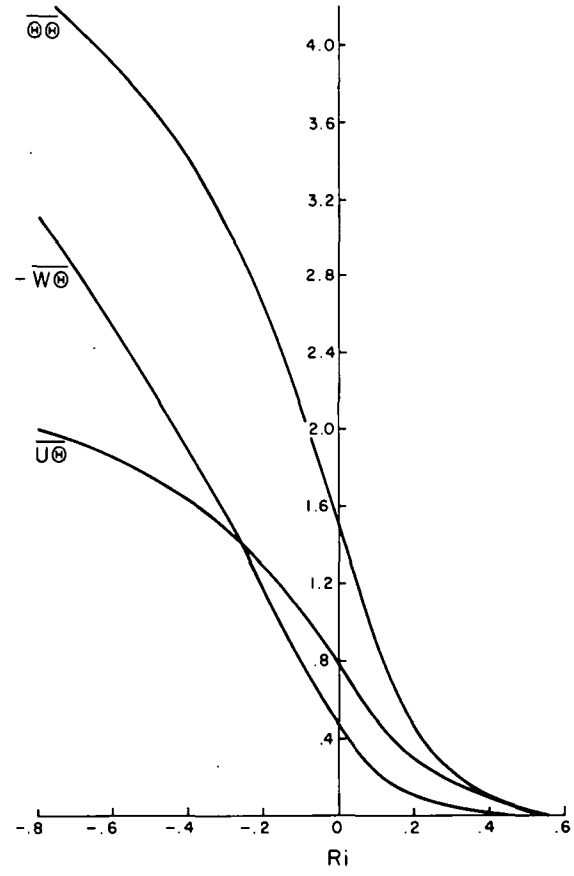

Fig. 5.1(b) Superequilibrium temperature correlation profiles normalized by $\Lambda^2(\partial\Theta/\partial z)(\partial U/\partial z)$, etc.

6. Applications

We believe the verifications of the model predictions made in Section 4 sufficiently accurate over a wide variety of conditions to justify detailed calculations of flow situations for which no detailed measurements are available. A.R.A.P. is currently applying the model to a number of such areas. A few interesting results of these applications are presented here. Progress is also being made on applications to other areas including: compressible boundary layers,[59] compressible shear layers,[60,61] three-dimensional isolated vortex,[62] chemically reacting wakes[63] and jets,[64] swirling flow in an annulus,[65]

and moisture in the atmospheric boundary layer.

6.1 Diurnal Variations in the Planetary Boundary Layer

Over homogeneous terrain, the atmospheric boundary layer may be considered a function of time and altitude only. The results of calculations for a fixed geostrophic wind and upper level temperature lapse rate with a cyclic surface heat flux approximating conditions over the Midwestern plains during summer[66] are presented in Reference 24. These results were obtained using the quasi-equilibrium approach outlined in Section 5.2 and the gross feature approach to the scale. The results presented here were obtained using the full equations. There is relatively little difference in the numerical results.

The predicted contours of constant turbulent fluctuations are presented in Figure 6.1 as a function of time and altitude.

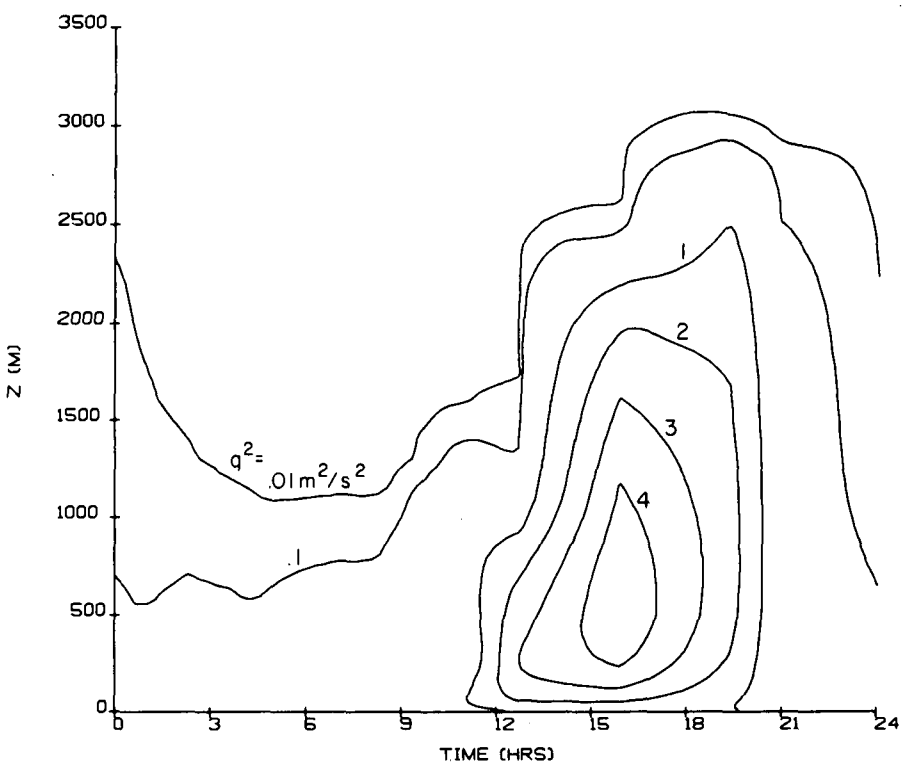

Fig. 6.1 Isopleths of turbulent energy in diurnal planetary boundary layer

The boundary layer thickness grows during the day and shrinks during the evening and morning hours. The turbulent kinetic energy reaches a maximum of 4.8% of the geostrophic mean kinetic energy in the midafternoon at an altitude of approximately 500 meters. As the sun sets, the turbulence begins to decay

until in the early morning hours the maximum kinetic energy is ≈ 0.25% of the mean kinetic energy. The biggest difference between the results presented here and those in Reference 24 occurs during the early morning hours. The full equations with a dynamic scale predict a slower decay of q^2 and consequently considerably larger q^2 in the altitude range from 100 m to 1 km in the morning hours. But even this larger value is still quite small compared with afternoon values. Both model representations predict such features as the temperature inversion and local wind jet observed to occur nocturnally at low levels.

Surface shear stress is plotted as a function of the stability variable $\kappa u^*/fL$ in Figure 6.2. Data points for $Ro \approx 10^7$, as taken from Tennekes' summary[67] are included on the plot. The model predictions show a hysteresis loop with the surface shear stress significantly larger when the surface heat flux is decreasing rather than increasing. The data show considerable scatter but tend to be biased towards the upper bound. The factor of two difference in u* at neutral conditions demonstrates the influence of unsteady dynamics on the atmospheric boundary layer.

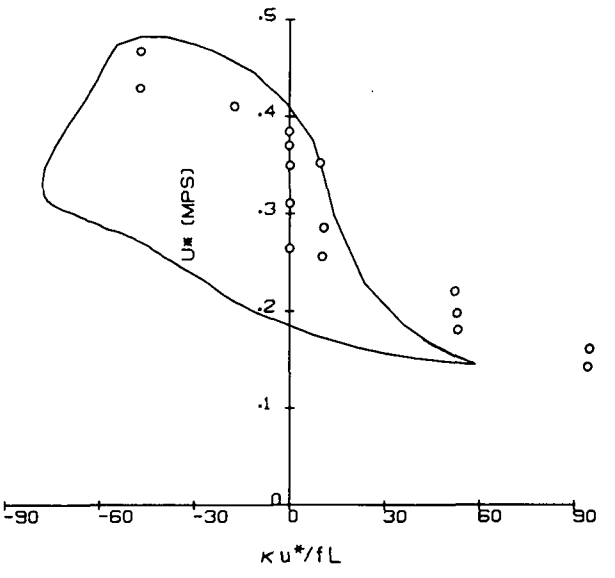

Fig. 6.2 Surface shear velocity vs. stability for diurnal planetary boundary layers. Data from Tennekes[67]

6.2 Stratified Wake

The passage of a body through a stratified fluid generates a turbulent wake containing kinetic and potential energy. The buildup of potential energy is caused by the co-mixing of

heavier density fluid above the lighter density fluid. In the initial stages of wake development in a weakly stratified medium, the turbulent kinetic energy dominates the potential energy, and the wake spreads. This spreading in turn increases the potential energy until, at a time comparable to the natural oscillating period of the fluid, inertial waves are generated. Computations for this flow using the quasi-equilibrium version of the present model have been reported in References 30 and 68.

Figure 6.3 shows typical contours of the turbulent kinetic energy and secondary flow stream function at two instances of time following wake initialization. Time is normalized by the characteristic Brunt-Väisälä period of the fluid

$$t_c = 2\pi[(g/\Theta)\partial\Theta/\partial z]^{-1/2}$$

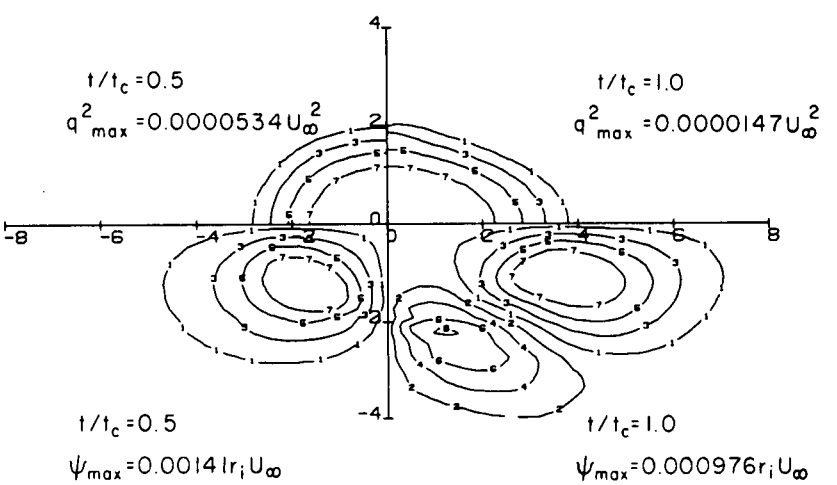

Fig. 6.3 Contours of turbulent energy and secondary flow streamlines for two instances of time after wake initialization for $Ri_0 = 0.00925$.
1 = +10% of maximum value for that quadrant;
2 = -10%; 3 = +30%; 4 = -30%, etc.

The flow is symmetric about both axes so only one quadrant is shown for each variable at each time. At $t/t_c = 0.5$, the secondary flow exhibits a simple collapsing motion, while at $t/t_c = 1$, a second wave mode has been added. At both times the secondary flow extends well outside the region of turbulence.

Figure 6.4 is a summary plot showing the sensitivity of the wake shape to initial Froude number, $F_D = Ut_c/D$, or initial Richardson number of the turbulence, $Ri_0 = (2\pi r_i/q_{max}t_c)^2$,

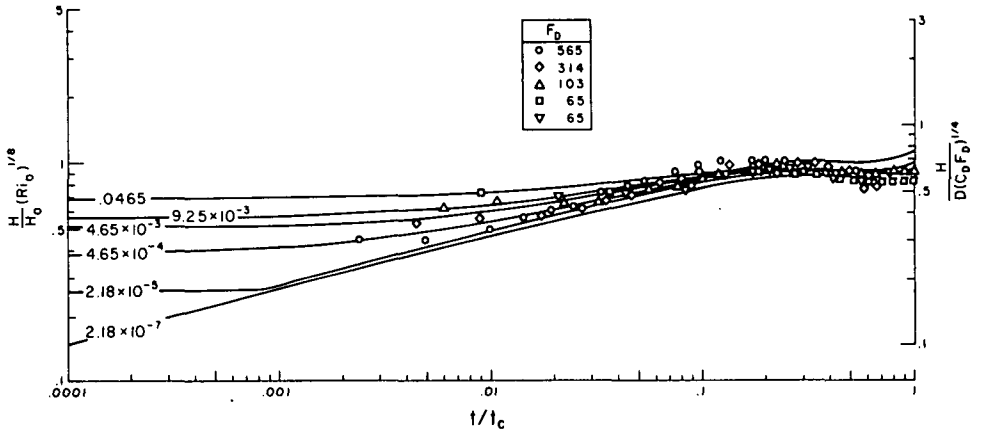

Fig. 6.4 Vertical spread of stratified wakes. Data from Lin and Pao[69]

along with a qualitative comparison with laboratory flow visualization results.[69] There is good qualitative agreement between the observations and predictions.

6.3 Pollutant Dispersal

By adding equations for species continuity C and the correlations of species fluctuations $\overline{u_i c}$, $\overline{cc}$, and $\overline{c\theta}$, (2.1)-(2.3) and (2.24)-(2.26) may be used to estimate pollutant dispersal in the atmospheric boundary layer. As long as the pollutant is assumed neutrally buoyant and nonreacting, the equations for C, $\overline{u_i c}$, $\overline{cc}$, and $\overline{c\theta}$ should be identical to (2.3), (2.25), and (2.26), respectively.

Results of computations of pollutant dispersal in atmospheric turbulence as represented by our model predictions have been presented in References 6, 29, and 70. Figure 6.5 shows the influence of atmospheric stability on the vertical spread σ_z of a plume released at ground level

$$\sigma_z^2 = \int_0^\infty (Cz^2)\, dz \Big/ \int_0^\infty C\, dz$$

The Richardson number $\hat{R}i$ is based on the difference between the values of temperature and velocity at 10 m altitude and at the surface, specifically,

$$\hat{R}i = \frac{g}{\Theta} \frac{\Delta\Theta_{10m}(1m)}{\hat{u}^2}$$

where $\hat{u} = 0.1U$ at 10 meters. The spread rate for neutral

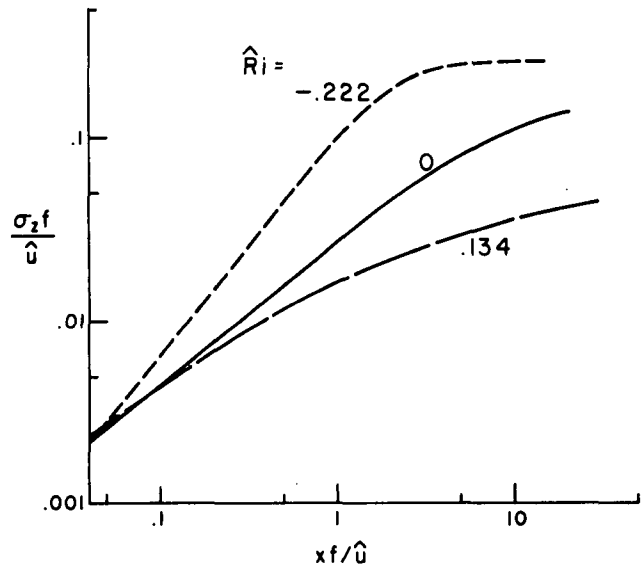

Fig. 6.5 Vertical plume spread from ground release into planetary boundary layers of various stabilities

conditions is very close to that predicted by Pasquill.[71] But the present model predicts a stronger effect of stability under unstable conditions and a weaker effect on the stable side.

Deardorff and Willis[72] have published results of particle releases into an unstable mixed layer, the same experimental flow used for comparison in Figures 4.15, 4.16, and 4.17. Reference 70 shows comparable model predictions for a surface pollutant released into the calculated, unstable-mixed layer field of turbulence shown in those figures. The model predicts that the maximum concentration will rise above the surface. As pointed out in Reference 72, this feature could not be predicted by any eddy viscosity model or a Gaussian plume model.

The model predicts several non-Gaussian features for pollutant plumes caused by such mechanisms as wind shear in magnitude and direction with altitude, interaction with the inversion layer capping the boundary layer, and regions where turbulent scales are much larger than plume scales.

7. Concluding Remarks

Second-order closure has been established as a viable approach to practical turbulent flow computations. There are still about as many models as there are modelers — each model differing from the others in some detail. But this is a

healthy situation, since there is still much to be learned. This is particularly true of the scale equation since in any of the models, every term is this equation must be modeled.

The relatively simple model presented here does a commendable job over a wide variety of flows. Thus, practical calculations can proceed concurrently with attempts to improve the model.

References

[1]Bradshaw, P., "The Understanding and Prediction of Turbulent Flows," Aeronautical Journal, 1972, pp. 403-418.

[2]Mellor, G.L. and Herring, H.J., "A Survey of Mean Turbulent Field Closure Models," AIAA Journal, Vol. 11, No. 5, May 1973, pp. 590-599.

[3]Reynolds, W.C., "Computation of Turbulent Flows — State-of-the-Art, 1970," Report MD-27, Dept. of Mech. Eng., Stanford University, 1970.

[4]Harlow, F.H. (Ed.), "Turbulence Transport Modeling," AIAA Selected Reprint Series, Vol. XIV, 1973.

[5]Phillips, O.M., The Dynamics of the Upper Ocean, Cambridge University Press, Cambridge, 1969.

[6]Donaldson, C.duP., "Atmospheric Turbulence and the Dispersal of Atmospheric Pollutants," AMS Workshop on Micrometeorology, edited by D. A. Haugen, Science Press, Boston, 1973, pp. 313-390; also EPA-R4-73-016a, March 1973.

[7]Tennekes, H. and Lumley, J.L., A First Course in Turbulence, MIT Press, Cambridge, 1972.

[8]Donaldson, C.duP., "Calculation of Turbulent Shear Flows for Atmospheric and Vortex Motions," AIAA Journal, Vol. 10, No. 1, January 1972, pp. 4-12.

[9]Daly, B.J. and Harlow, F.H., "Transport Equations in Turbulence," Physics of Fluids, Vol. 13, No. 11, November 1970, pp. 2634-2649.

[10]Wolfshtein, M., Naot, D., and Lin, A., "Models of Turbulence," Ben-Gurion University of the Negev Report ME-746(N), 1974.

[11]Rotta, J.C., "Statistiche Theorie nichthomogener Turbulenz," Z. Physik, Vol. 129, 1951, pp. 547-572.

[12]Rotta, J.C., Turbulente Strömungen, B.G. Teubner, Stuttgart, 1972.

[13]Crow, S.C., "Viscoelastic Properties of Fine-Grained Incompressible Turbulence," J. Fluid Mechanics, Vol. 33, Part 1, 1968, pp. 1-20.

[14]Launder, B.E. and Spalding, D.B., Mathematical Models of Turbulence, Academic Press, New York, 1972.

[15]Rodi, W., "The Prediction of Free Turbulent Boundary Layers by Use of a Two-Equation Model of Turbulence," Dissertation submitted to Mechanical Engineering Dept., Imperial College, London, December 1972.

[16]Mellor, G.L., "Analytic Prediction of the Properties of Stratified Planetary Surface Layers," Journal of Atmospheric Sciences, Vol. 30, 1973, pp. 1061-1069.

[17]Launder, B.E., "On the Effects of a Gravitational Field on the Turbulent Transport of Heat and Momentum," J. Fluid Mechanics, Vol. 67, Part 3, 1975, pp. 569-581.

[18]Naot, D., Shavit, A. and Wolfshtein, M., "Two-Point Correlation Model and the Redistribution of Reynolds Stresses," Physics of Fluids, Vol. 16, No. 6, 1973, pp. 738-743.

[19]Lumley, J.L. and Khajeh-Nouri, B., "Computational Modeling of Turbulent Transport," Advances in Geophysics, Vol. 18A, Academic Press, New York, 1974.

[20]Hanjalic, K. and Launder, B.E., "A Reynolds Stress Model of Turbulence and Its Application to Asymmetric Boundary Layers," J. Fluid Mechanics, Vol. 52, No. 4, 1972, pp. 609-638.

[21]Zeman, D. and Tennekes, H., "A Self-Contained Model for the Pressure Terms in the Turbulent Stress Equations of the Atmospheric Boundary Layer," unpublished manuscript, 1975.

[22]Varma, A.K., "Second-Order Closure of Turbulent Reacting Shear Flows," A.R.A.P. Report No. 235, February 1975.

[23]Lewellen, W.S., Teske, M. and Donaldson, C.duP., "Application of Turbulent Model Equations to Axisymmetric Wakes," AIAA Journal, Vol. 12, No. 5, 1974, pp. 620-625.

[24]Lewellen, W.S., Teske, M. and Donaldson, C.duP., "Turbulence Model of Diurnal Variations in the Planetary Boundary Layer," Proc. 1974 Heat Transfer and Fluid Mechanics Institute, edited by L.R.Davis and R.E.Wilson, Stanford University Press, Stanford, 1974, pp. 301-319.

[25]Shir, C.C., "A Preliminary Numerical Study of Atmospheric Turbulent Flows in the Idealized Planetary Boundary Layer," J. Atmospheric Sciences, Vol. 30, 1973, pp. 1327-1339.

[26]Mellor, G.L. and Yamada, T., "A Hierarchy of Turbulence Closure Models for Planetary Boundary Layers," J. Atmospheric Sciences, Vol. 31, 1974, pp. 1791-1806.

[27]Harlow, F.H. and Nakayama, P.I., "Turbulence Transport Equations," Physics of Fluids, Vol. 10, No. 11, 1967, pp. 2323-2332.

[28]Wilcox, D.C. and Alber, I.E., "A Turbulence Model for High Speed Flows," Proc. 1972 Heat Transfer and Fluid Mechanics Institute, Stanford University Press, Stanford, 1972, pp. 231-252.

[29]Lewellen, W.S., Teske, M., Contiliano, R.M., Hilst, G.R.,and Donaldson, C.duP., "Invariant Modeling of Turbulent Diffusion in the Planetary Boundary Layer," EPA-650/4-74-035, September 1974.

[30]Lewellen, W.S., Teske, M., and Donaldson, C.duP., "Turbulent Wakes in a Stratified Fluid," A.R.A.P. Report No. 226, September 1974.

[31]Champagne, F.H., Harris, V.G., and Corrsin, S., "Experiments on Nearly Homogeneous Turbulent Shear Flows," J. Fluid Mechanics, Vol. 41, Part 1, 1970, pp. 81-139.

[32]Businger, J.A., Wyngaard, J.C., Izumi, Y., and Bradley, E.F., "Flux-Profile Relationships in the Atmospheric Surface Layer," J. Atmospheric Sciences, Vol. 28, 1971, pp. 181-189.

[33]Gad-el-Hak, M. and Corrsin, S., "Measurements of the Nearly Isotropic Turbulence Behind a Uniform Jet Grid," J. Fluid Mechanics, Vol. 62, Part 1, 1974, pp. 115-143.

[34]Coles, D., "Measurements in the Boundary Layer on a Smooth Flat Plate in Supersonic Flow. Part I: The Problem of the Turbulent Boundary Layer," JPL Report 20-69, 1953.

[35]Gibson, C.H., Stegen, G.R., and Williams, R.B., "Statistics of the Fine Structure of Turbulent Velocity and Temperature Fields Measured at High Reynolds Number," J. Fluid Mechanics, Vol. 41, Part 1, 1970, pp. 153-167.

[36]Lewellen, W.S. and Teske, M.E., "Prediction of the Monin-Obukhov Similarity Functions from an Invariant Model of Turbulence," J. Atmospheric Sciences, Vol. 30, 1973, pp. 1340-1345.

[37]Wyngaard, J.C., Coté, O.R., and Rao, K.S., "Modeling the Atmospheric Boundary Layer," Advances in Geophysics, Vol. 18A, Academic Press, New York, 1974.

[38]Wyngaard, J.C. and Coté, O.R., "The Evolution of a Convective Planetary Boundary Layer - A Higher-Order Closure Model Study," Boundary Layer Meteorology, Vol. 7, 1974, p. 289.

[39]Wygnanski, I. and Fiedler, H., "Some Measurements in the Self-Preserving Jet," J. Fluid Mechanics, Vol. 38, Part 3, 1969, pp. 577-612

[40]Wygnanski, I. and Fiedler, H., "The Two-Dimensional Mixing Region," J. Fluid Mechanics, Vol. 41, Part 1, 1970, pp. 327-361.

[41]Birch, S.F. and Eggers, J.M., "A Critical Review of the Experimental Data for Developed Free Turbulent Shear Layers," Free Turbulent Shear Flows, Volume I (also see Volume II, Summary of Data), NASA SP-321, 1973.

[42]Townsend, A.A., The Structure of Turbulent Shear Flow, Cambridge University Press, Cambridge, 1956.

[43]Thomas, R.M., "Conditional Sampling and Other Measurements in a Plane Turbulent Wake," J. Fluid Mechanics, Vol. 57, Part 3, 1973, pp. 549-582.

[44]Chevray, R., "The Turbulent Wake of a Body of Revolution," Journal of Basic Engineering, Vol. 90, Series E, 1968, pp.275-284.

[45]Naudascher, R., "Flow in the Wake of Self-Propelled Bodies and Related Sources of Turbulence," J. Fluid Mechanics, Vol.22, Part 4, pp. 625-656.

[46]Klebanoff, P.S., "Characteristics of Turbulence in a Boundary Layer with Zero Pressure Gradient," NACA Report 1247, 1954.

[47]Bradley, E.F., "A Micrometeorological Study of Velocity Profiles and Surface Drag in the Region Modified by a Change in Surface Roughness," Quart. J. Royal Meteorol. Soc, Vol. 94, 1968, pp. 361-379.

[48]Rao, K.S., Wyngaard, J.C., and Coté, O.R., "The Structure of Two-Dimensional Internal Boundary Layer Over a Sudden Change of Surface Roughness," J. Atmospheric Sciences, Vol. 31, 1974, pp. 738-746.

[49]Freymuth, P. and Uberoi, M.S., "Structure of Temperature Fluctuations in the Turbulent Wake Behind a Heated Cylinder," Physics of Fluids, Vol. 14, No. 12, 1971, pp. 2574-2580.

[50]LaRue, J.C. and Libby, P.A., "Temperature Fluctuations in the Plane Turbulent Wake," Physics of Fluids, Vol. 17, No. 11, 1974, pp. 1956-1975.

[51]Monin, A.S. and Obukhov, A.M., "Dimensionless Characteristics of Turbulence in the Atmospheric Surface Layer," Dokl. Akad. Nauk, SSSR, Vol. 93, 1953, pp. 223-226.

[52]Wyngaard, J.C., Coté, O.R., and Izumi, Y., "Local Free Convection, Similarity, and the Budgets of Shear Stress and Heat Flux," J. Atmospheric Sciences, Vol. 28, 1971, pp. 1171-1182.

[53]Kato, H. and Phillips, O.M., "On the Penetration of a Turbulent Layer into Stratified Fluid," J. Fluid Mechanics, Vol.37, No. 4, 1969, pp. 643-656.

[54]Willis, G.E. and Deardorff, J.W., "A Laboratory Model of the Unstable Planetary Boundary Layer," J. Atmospheric Sciences, Vol. 31, 1974, pp. 1297-1307.

[55]Deardorff, J.W., "Numerical Investigation of Neutral and Unstable Planetary Boundary Layers," J. Atmospheric Sciences, Vol. 29, 1972, pp. 91-115.

[56]Donaldson, C.duP., "The Relationship Between Eddy Transport and Second-Order Closure Models for Stratified Media and for Vortices," Free Turbulent Shear Flows, Volume I, NASA SP-321, 1973,pp. 233-255.

[57]Donaldson, C. duP. and Bilanin, A.J., "Vortex Wakes of Conventional Aircraft," AGARDograph No. 204 (in press).

[58]Mellor, G.L., "A Comparative Study of Curved Flow and Density Stratified Flow," unpublished manuscript, 1974.

[59]Donaldson, C.duP. and Sullivan, R.D., "An Invariant Second-Order Closure Model of the Compressible Turbulent Boundary Layer on a Flat Plate," A.R.A.P. Report No. 178, 1972.

[60]Varma, A.K., Beddini, R.A., Sullivan, R.D., and Donaldson, C.duP., "Application of an Invariant Second-Order Closure Model to Compressible Turbulent Shear Layers," AIAA Paper No. 74-592, June 1974, Palo Alto.

[61]Varma, A.K., Beddini, R.A., Sullivan, R.D., and Fishburne, E.S., "Turbulent Shear Flows in Laser Nozzles and Cavities," AFOSR-TR-74-1786, October 1974.

[62]Sullivan, R.D., "A Program to Compute the Behavior of a Three-Dimensional Turbulent Vortex," ARL-TR-74-0009, 1973.

[63]Hilst, G.R., "The Chemistry and Diffusion of Aircraft Exhausts in the Lower Stratosphere During the First Few Hours After Flyby," A.R.A.P. Report No. 216, May 1974.

[64]Donaldson, C.duP. and Varma, A.K., "Remarks on the Construction of a Second-Order Closure Description of Turbulent Reacting Flows," Combustion Science and Technology (in press).

[65]Bilanin, A.J., Snedeker, R.S., Sullivan, R.D., and Donaldson, C.duP., "Final Report on An Experimental and Theoretical Study of Aircraft Vortices," A.R.A.P. Report No. 238, 1975.

[66]Wyngaard, J.C., "Notes on Surface Layer Turbulence," AMS Workshop on Micrometeorology, edited by D.A. Haugen, Science Press, Boston, 1973, pp. 101-149.

[67]Tennekes, H., "Similarity Laws and Scale Relations in Planetary Boundary Layers," AMS Workshop on Micrometeorology, edited by D.A. Haugen, Science Press, Boston, 1973, pp. 177-216.

[68]Lewellen, W.S., Teske, M. and Donaldson, C.duP., "Second-Order, Turbulent Modeling Applied to Momentumless Wakes in Stratified Fluids," A.R.A.P. Report No. 206, 1973.

[69]Lin, J.T. and Pao, Y.H., "Turbulent Wake of a Self-Propelled Slender Body in Stratified and Nonstratified Fluids: Analysis and Flow Visualizations," Flow Research Corp. Report No. 11, 1973.

[70]Lewellen, W.S. and Teske, M., "Second-Order Closure Modeling of Diffusion in the Atmospheric Boundary Layer," A.R.A.P. Report No. 242, April 1975.

[71]Pasquill, F., Atmospheric Diffusion, 2nd edition, Halstead Press, John Wiley & Sons, Inc., New York, 1974.

[72]Deardorff, J.W. and Willis, G.E., "Physical Modeling of Diffusion in the Mixed Layer," Proc. Symposium on Atmospheric Diffusion and Air Pollution, Santa Barbara, September 1974, American Meteorological Society, Boston, pp. 387-391.

NOMENCLATURE

A, a, b	model constants
C	mean species concentration
c	species concentration fluctuations about the mean
D	laminar diffusion coefficient
d	model constant relating plume spread to plume turbulent scale, see Eq. (15)
f	Coriolis parameter = $2\Omega \sin \phi$
g	gravitational acceleration
k	von Karman's constant = $-u^*/(z\ \partial u/\partial z)_o$ in the neutral surface layer
L	Monin-Obukhov length = $-\Theta_o u^{*3}/kg(\overline{w\theta})_o$
n	decay rate for grid turbulence
P	mean pressure (also Pasquill's stability parameter)
p	pressure fluctuation
q	square root of twice the turbulent kinetic energy
Q	source strength
Ri	Richardson number
$\hat{Ri}$	characteristic Richardson number defined in Eq. (12)
Ro	Rossby number based on geostrophic conditions = U_g/fz_o
$\hat{Ro}$	characteristic Rossby number = $\hat{u}/fz_o$
s	model constant
s_0, s_1, s_2	constants in scale equation
t	time
t_c	Brunt-Väisälä period
U_i	mean fluid velocity in the ith direction
U_g	geostrophic wind velocity
u_i	fluctuating fluid velocity in the ith direction
u^*	surface shear stress velocity

$\hat{u}$	characteristic surface velocity equal to 0.1 times the wind velocity at 10 meters
v_c	model turbulent diffusion coefficient
W	mean vertical velocity
w	fluctuating vertical velocity
w^*	free convective velocity scale = $[gz_i(\overline{w\theta})_o/\Theta_o]^{1/3}$
x_i, x_j, x_k	Cartesian coordinates
z	vertical coordinate
z_i	temperature inversion height above an unstable layer
z_o	surface roughness height
z_{50}	distance to 1/2 the centerline value
z_r	plume release height
ε	dissipation function
Θ	mean potential temperature
θ	fluctuating potential temperature
Λ	model macroscale length
λ	model microscale length = $\Lambda/[a + bq\Lambda/\nu]^{1/2}$
ν	kinematic viscosity
ρ	density
ϕ	latitude
Ω_i	angular velocity of the coordinate system
σ	plume spread

Superscript:

$\overline{}$	denotes ensemble average

Subscript:

o	denotes surface value
g	denotes geostrophic condition
p	denotes plume value
t	denotes ambient turbulence value